THE JOURNAL OF PHYSICAL CHEMISTRY A

Article

pubs.acs.org/JPCA

Mercury Oxidation via Chlorine, Bromine, and Iodine under Atmospheric Conditions: Thermochemistry and Kinetics

Itsaso Auzmendi-Murua, Álvaro Castillo, and Joseph W. Bozzelli*

Department of Chemistry and Chemical Engineering, New Jersey Institute of Technology, Newark, New Jersey 07102, United States

Supporting Information

ABSTRACT: Emissions of gaseous mercury from combustion sources are the major source of Hg in the atmosphere and in environmental waters and soils. Reactions of $Hg^{o}(g)$ with halogens are of interest because they relate to mercury and ozone depletion events in the Antarctic and Arctic early spring ozone hole events, and the formation of Hg-halides (HgX_2) is a method for removal of mercury from power generation systems. Thermochemistry and kinetics from published theoretical and experimental studies in the literature and from computational chemistry are utilized to compile a mechanism of the reactions considered as contributors to the formation of HgX_2 (X = Cl, Br, I) to understand the reaction paths and mechanisms under atmospheric conditions. Elementary reaction mechanisms are assembled and evaluated using thermochemistry for all species and microscopic reversibility for all reactions. Temperature and pressure dependence is determined with quantum Rice Ramsperger Kassel (RRK) analysis for $k(E)$ and master equation analysis for fall-off. We find that reactions of mercury with a small fraction of the reactor surface or initiation by low concentrations of halogen atoms is needed to explain the experimental conversion of Hg to HgX_2 in the gas phase. The models do not replicate data from experiments that do not explicitly provide an atom source. The Hg insertion reaction into X_2 ($Hg + X_2 \rightarrow HgX_2$) that has been reported is further studied, and we find agreement with studies that report high barriers. The high barriers prevent this insertion path from explaining the experimental data on HgX_2 formation and Hg conversion under atmospheric conditions. Mechanism studies with low initial concentrations of halogen radicals show significant conversion of Hg under the experimental conditions.

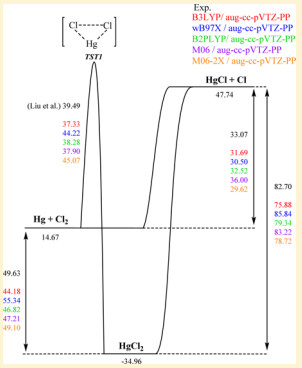

INTRODUCTION

The adverse effects of mercury in the environment have been known for years; however, it has only been in recent years that regulation of mercury has been significantly implemented. In March 2005 the U.S. Environmental Protection Agency (EPA) regulated mercury emissions from coal-fired power plants, when issuing the Clean Air Mercury Rule (CAMR), which created the first performance standards and established permanent, declining caps in mercury emissions. On December 21, 2011, EPA announced standards to limit mercury emissions from electricity generating plants.[1] In January 2013, 140 nations adopted the first legally binding international treaty to set enforceable limits on emissions of mercury and exclude, phase out, or restrict some products that contain mercury.

Although mercury is present in coal and municipal solid wastes in only minute amounts, on the order of 0.1 ppm_w,[2] 458.6 tons of mercury are emitted worldwide each year from power generating plants, 63.1 tons being emitted in North America and 241.1 tons in Asia and Oceania as of 2009.[3] Mercury is among the most highly bioconcentrated trace metals in the human food chain.[4] Once mercury is deposited on land or into water, it is transformed by microorganisms into methylmercury (II) ($[CH_3Hg]^+$) and dimethylmercury ($Hg(CH_3)_2$), an organic form of mercury, which is a potent neurotoxin.[5,6] Elemental mercury, $Hg^{\circ}(g)$, is also observed to decrease along with the ozone in the Antarctic and Artic early spring ozone hole events, and its chemistry may likely be related to reactions with halogens and halogen oxides, e.g., chlorine atoms and ClO_x radicals.[7,8]

Both experimental and theoretical studies suggest that the gas phase recombination of Hg° with halogen atoms is sufficiently fast to initiate the oxidation process of mercury. The available experiments state that the diurnal cycle of reactive gaseous mercury (RGM) in surface air suggests that the oxidation of mercury must be photochemical. However, there is a large uncertainty in the value of the rate coefficient for this recombination reaction and in the fate of the reaction product, HgX (X = Cl, Br, I).[9−15]

There are several early experimental studies focused on the halogenation chemistry of mercury under ambient or near ambient conditions. In 1936 Ogg et al.[16] performed experiments at 1 atm and 383 K to study the oxidation reactions between Hg and Br_2. They concluded that the mechanism involving reactions ($Hg + Br_2 \rightarrow HgBr + Br$) and ($HgBr + Br_2 \rightarrow HgBr_2 + Br$) play no appreciable role and that the observed mercury−bromine reaction is due to the association (insertion) reaction ($Hg + Br_2 \rightarrow HgBr_2$). They assumed that the reaction $Hg + Br_2 \rightarrow HgBr_2$ occurs only on collision with a third body, concluding a rate constant of 4×10^{10} cm^6 mol^{-2} s^{-1}. In 1949 P'yankov et al.[17] published experimental results studying

Received: December 26, 2013
Revised: March 22, 2014

   dx.doi.org/10.1021/jp412654s | J. Phys. Chem. A XXXX, XXX, XXX−XXX

the reaction of Hg and Cl_2 at 1 atm, concluding that the main product was Hg_2Cl_2 but that the $HgCl_2$ concentration increased slowly when increasing the Hg/Cl ratio. Menke and Wallis[18] presented experimental results, where mercury vapor and chlorine gas were combined. They suggested the product may be $HgCl_2$. Hall et al.[19] published experimental results where Hg oxidation was studied with and without Cl_2 present. They did not report any rate constants. Fontijn and Hranisavljevic[20] published higher temperature experimental data on the rate constants for the reaction between Hg and Cl_2. They stated that there was no experimental evidence for association or insertion reactions and suggested that the reaction $Hg + Cl_2 \rightarrow HgCl + Cl$ would not proceed at measurable rates under normal combustion conditions. They do not discuss a direct insertion reaction of Cl_2 in mercury. Our findings below are in agreement with the results of Fontijn and Hranisavljevic.

Using Menke and Wallis' experimental results,[18] Schroeder et al.[21] calculated a rate constant, providing an upper limit of 2.4×10^8 cm^3 mol^{-1} s^{-1}. However, they stated that the actual reaction is not entirely described by $Hg + Cl_2 \rightarrow HgCl_2$. Experimental data on Hg conversion with chlorine were published by Kramlich et al. in 2000.[22] They indicated the product of the direct reaction could be $HgCl_2$ and provided a rate constant of 3.4×10^9 cm^3 mol^{-1} s^{-1}, for temperatures between 293 and 973 K. One year later Edwards et al.[23] constructed a reaction mechanism that they simulated with the CHEMKIN-III package,[24] to compare model results with experimental data.

Ariya et al.[25,26] performed experiments to study the oxidation of mercury by chlorine, bromine, and iodine, at 1 atm and 298 ± 1 K. Reactions of mercury with molecular halogens were studied using 0.5−10 ppm mercury, 10−50 ppm Cl_2 and Br_2, and 130 ppm I_2. They stated that for $Hg + X_2$ (X = Cl, Br, I) reactions, the major products identified were $HgCl_2$, $HgBr_2$, and HgI_2. Chang et al. carried out vapor phase experiments[27,28] to study the oxidation of mercury by chlorine and bromine respectively at 297 ± 1 K and 1 atm. They also studied the difference in loss of Hg using a pulsed vs continuous source of the absorption (Hg line) for evaluation of photoinduced reactions. In 2005 they published[28] a rate constant for the oxidation reaction of mercury by Cl_2 and indicated that the gas phase reaction of Hg and Cl_2 can be regarded as a three-body reaction ($Hg + Cl_2 + M \rightarrow HgCl_2 + M$). In 2007 they published[27] their experimental calculations for the oxidation of mercury by bromine under atmospheric conditions where the kinetics changed with both surface to volume ratio and with pulsed versus continuous source operation. We interpret their pulsed light source data as excitation of the Hg having a significant acceleration effect on the kinetics.

Yan et al.[29,30] reported experimental data for the oxidation of mercury by chlorine, bromine, iodine, bromine chloride, and iodine chloride at 1 atm and 373 K. They do not report a numerical rate constant for Cl_2, Br_2, and I_2, but they do report a plot with the oxidation of Hg by Cl_2, Br_2, and I_2 addition (experimental C/C_o versus time). Numerical values for the rate constants for Br_2, Cl_2, and I_2 were estimated in this work as 2.62×10^7, 1.67×10^6, and 1.20×10^8 cm^3 mol^{-1} s^{-1}, respectively. A summary of reported experimental data by Yan et al. of C/C_o versus time, and the rate constants calculated in this work for reactions of mercury with chlorine and bromine versus time are presented in the Supporting Information.

In 2003, Ariya et al.[31] reported rate constants for the reactions $Hg + X \rightarrow HgX$ (X = Cl, Br). They considered the direct insertion reactions and calculated the reaction enthalpy but did not report rate constants evaluation for the reactions.

Goodsite et al.[12] studied the oxidation of Hg to $HgBr_2$ under conditions relevant to the troposphere using computational chemistry (at B3LYP/CEP-121G level of theory). They provided rate constants for the reactions $Hg + Br \rightarrow HgBr$ and $HgBr + Br \rightarrow HgBr_2$, but they did not report details on Hg association with or insertion to Br_2. The work by Goodsite et al.[12] also provided data for the oxidation of mercury with iodine.

In 2005 Peterson et al.[8] carried out high level icMRCI+Q theoretical calculations for the insertion reaction, $Hg + Br_2 \leftrightarrow HgBr_2$, by microcanonical variational transition state theory. They reported a high value for the energy of activation at 27.2 kcal/mol and a rate constant of 1.65×10^{-7} cm^3 mol^{-1} s^{-1} at 298 K. That same year, Peterson et al.[32] published on the energetics of I_2, HgI, and HgI_2, but no kinetic parameters were reported. The research group of Wilcox[33] evaluated the reaction kinetics on $Hg + Cl_2$ reacting through a linear Hg···Cl−Cl complex to HgCl + Cl products, using a basis set that employs a relativistic compact effective potential, B3LYP/RCEP60 VDZ of the Stevens et al. group[34] and transition state theory. They calculated a rate constant of $6.15 \times 10^{13} \exp(-43.3/RT)$ cm^3 mol^{-1} s^{-1} (Ea, kcal mol^{-1}). In a more recent work,[35] Wilcox and Okano studied the reaction between Hg and Br_2 to products HgBr + Br at the same level of theory; they reported a rate constant of $1.15 \times 10^{15} \exp(-30.1/RT)$ cm^3 mol^{-1} s^{-1} . We note that these reactions are endothermic by 33 and 29.5 kcal mol^{-1}, respectively. They do not report on the insertion reaction but comment that the direct insertion reaction is not likely to occur because of the high energy of activation. Liu et al.[36] recently provided the rate expressions for several reactions involving mercury. For the direct insertion reaction of mercury in molecular chlorine, they estimated an energy of activation of 39.49 kcal mol^{-1} and a preexponential factor of 1.04×10^{14} cm^3 mol^{-1} s^{-1}.

A more detailed description of the discussed literature results is present in the Supporting Information.

The implications of computational studies by the research groups of Peterson,[8] Wilcox,[33,35] and Liu[36] all infer a sequence of reactions forming the stable HgX_2 (X = Cl or Br) that does not involve a direct reaction of $Hg + X_2$ to form HgX_2. They all suggest a reaction sequence that requires radical halogen species.

$$Hg + X + (M) \rightarrow HgX + (M)$$

$$Hg + X_2 \rightarrow HgX + X$$

$$HgX + X_2 \rightarrow HgX_2 + X$$

While the focus of this study is on low temperature reactions of mercury with the halogens, we need to indicate that a number of studies[37−45] have been reported on the conversion of mercury at higher temperatures, typical of combustion conditions. A number of these studies involve kinetic reaction sequences or mechanisms, where the kinetics may also be relevant to lower temperature systems. The early work is by Widmer et al. who presented an eight step elementary reaction sequence for the formation of $HgCl_2$ from Hg° and chlorine-containing species.[43,44] Niksa et al.[39] further developed the eight step reaction mechanism proposed by Widmer et al.,[44] and more recently Fry et al.[37] have performed experimental studies on the conversion of mercury by bromine and chlorine at conditions typical of combustion effluent environments.

dx.doi.org/10.1021/jp412654s | J. Phys. Chem. A XXXX, XXX, XXX−XXX

It is appropriate to review or emphasize that the bond energies of Hg−Cl, Hg−Br, and Hg−I are quite weak (24.9, 13.5, and 8.3 kcal mol^{-1} respectively, gas phase). These important intermediates are borderline stable at atmospheric conditions and unstable at combustion and incinerator effluent temperatures. The enthalpy of formation and bond energies of each of the species are summarized in Table 1.

Table 1. Enthalpies of Formation and Bond Energies (kcal mol^{-1}) at 298 K, Gas Phase[a]

species	$\Delta_f H°(298)$ (kcal mol^{-1})	bond energy (kcal mol^{-1})	ref.
Hg	14.67		47
Cl	28.99		47
Br	26.74		47
I	25.52		47
Cl_2	0.00	57.98	47
Br_2	7.39	46.09	47
I_2	14.92	−36.12	47
HgCl	18.75	24.91	7
HgBr	24.88	16.53	7
HgI	31.90	−8.29	47
$HgCl_2$	−34.96	82.70	7
$HgBr_2$	−20.42	72.62	7
HgI_2	−3.86	−61.28	47

[a]HgX_2 bond energies are for the HgX—X bond, the second Hg—X bond in the structure.

Table 2. Enthalpies of Reaction of the Studied Hg/Cl, Hg/Br, and Hg/I Reactions

	ΔH_{reacn} (kcal mol^{-1})		
reacn	Cl	Br	I
Hg + X ↔ HgX	−24.91	−13.53	−8.29
HgX + X_2 ↔ HgX_2 + X	−24.72	−25.95	−25.16
Hg + X_2 ↔ HgX + X	33.07	29.56	27.83
HgX + X ↔ HgX_2	−82.70	−72.04	−61.28
Hg + X_2 ↔ HgX_2	−49.63	−42.48	−33.45

The possible reactions between mercury and the halogens are summarized in Table 2, each with the corresponding heat of reaction. The reactions Hg + X → HgX are exothermic (−24.9, −13.5, and −8.3 kcal mol^{-1} respectively for Cl, Br, and I), and could occur at atmospheric temperature, but require an initial reaction of halogen atoms. The reactions of Hg with Cl_2, Br_2, and I_2 to the corresponding HgX + X are endothermic (33.1, 29.6, and 27.8 kcal mol^{-1} respectively for Cl, Br, and I) and will not occur under atmospheric conditions, unless Hg or the halogens are in an excited state. The insertion reactions of Hg with halogen molecules to HgX_2 are exothermic (−49.6, −42.5, and −33.5 kcal mol^{-1}, respectively) but are predicted to have significant barriers (39.5 and 27.2 kcal mol^{-1} for chlorine and bromine, respectively), which preclude HgX_2 formation under atmospheric conditions (see Table 3). It is, therefore, difficult to justify the formation of HgX_2 observed by experimental studies under atmospheric conditions with the current available literature thermochemical and kinetic data. There are three scenarios that could justify the loss of Hg observed experimentally: (i) the conversion of mercury occurs through heterogeneous reactions on the walls of the reactor; (ii) there is a source of halogen atoms in the experiments; (iii) the insertion reaction, Hg + X_2 → HgX_2, is more important than previously predicted. A number of the earlier studies also infer that a direct

Table 3. Rate Constants from Theoretical Literature Calculations for Hg + X_2, at 298 K

reacn	energy of activation (kcal mol^{-1})	rate constant (cm^3 mol^{-1} s^{-1})	ref
Hg + Cl_2 ↔ $HgCl_2$	39.49	1.13×10^{-15}	36
Hg + Br_2 ↔ $HgBr_2$	27.2	1.65×10^{-7}[a]	8

[a]The reported value is 2.7×10^{-31} cm^3 mol^{-1} s^{-1}, but we assume the units are cm^3 $molecule^{-1}$ s^{-1}.

Hg + X_2 → HgX_2 path may occur,[8,33,35,36] but there are uncertainties on the height of the barriers. In the atmospheric temperature and pressure environment of the reaction studies discussed just above, the presence of atom sources is usually not considered because the experiments did not have a source.

If there would be a source or reaction to form the Cl, Br, or I atoms, the reactions Hg + X → HgX could rapidly happen. Once HgCl, HgBr, or HgI is formed, it is sufficiently long-lived that further reactions with halogen molecules or atoms can form the more stable $HgCl_2$, $HgBr_2$, and HgI_2. The HgX reaction with halogen atoms to form HgX_2 is exothermic (−82.7, −72.0, and −61.3 kcal mol^{-1} for Cl, Br, and I, respectively). The HgX reactions with halogen molecules to form HgX_2 + X are also exothermic (−24.7, −25.9, and −25.2 kcal mol^{-1} for Cl, Br, and I systems, respectively). The exothermicity comes from the stronger XHg—X bond relative to the Hg—X bonds.

A detailed reaction mechanism for the description of the atmospheric oxidation of mercury, based on fundamental principles of thermochemistry and statistical mechanics, is assembled in this work. The constructed mechanism is used for comparison with the available literature experimental data. Further calculations on the direct insertion reaction (Hg + X_2 → HgX_2) are performed, since the reactions present some uncertainties. We utilize a number of calculation methods and several basis sets and compare properties of reference species with literature values for evaluation of calculation method accuracy.

COMPUTATIONAL METHODS

Thermodynamic Properties. The thermochemical properties heats of formation, entropies, and heat capacities are determined from evaluation of literature data, from the published values by the research groups of Peterson,[7,46] Goodsite,[12] and Dibble[11] and from our calculations. Enthalpies of atoms are from the National Institute of Standards and Technology (NIST).[47] Table 1 summarizes the heats of formation (at 298 K) of the species used in these reaction systems, including the literature reference. The Supporting Information (Table S2) provides data on the entropy and heat capacity versus temperature for each of the species.

We have calculated transition state structures and energies, at several levels of theory; the transition state data are used primarily for preexponential kinetic factors. Thermochemical properties for the species involved in the direct insertion reaction have been obtained using the B3LYP, ωB97X, B2PLYP, M06, and M06-2X levels of theory, and three different basis sets, LANL2DZ, SDD, and aug-cc-pVTZ-PP. Single point calculations were performed at the higher level CCSD(T), with the use of the aug-cc-pVTZ-PP basis set.

The B3LYP method combines the three parameter Becke exchange functional, B3, with the Lee−Yang−Parr correlation functional, LYP.[48] In 1997, another significant advance in density functional theory (DFT) was made by Becke, who proposed to model exchange correlation functionals by a systematic

dx.doi.org/10.1021/jp412654s | J. Phys. Chem. A XXXX, XXX, XXX−XXX

Table 4. Rate Constants from Experimental Conversion of Hg (Hg + Cl_2) from the Literature

conditions	rate constant (cm^3 mol^{-1} s^{-1})	ref
	$Hg + Cl_2 \leftrightarrow HgCl_2$	
	2.4×10^8	21
1 atm, 293−973 K	3.4×10^9	22
1 atm, 298 ± 1 K, 0.5−10 ppm Hg, 10−50 ppm Cl_2	$(1.6 \pm 0.2) \times 10^6$	25
1 atm, 296 K, 0.16 ppm Hg, 242 ppm Cl_2	$(1.7 \pm 0.2) \times 10^5$	28
1 atm, 373 K, 0.16 ppm Hg, 10 ppm Cl_2	1.67×10^5	29

Table 5. Rate Constants from Experimental Conversion of Hg (Hg + Br_2) from the Literature

conditions	rate constant (cm^3 mol^{-1} s^{-1})	ref
	$Hg + Br_2 \leftrightarrow HgBr_2$	
1 atm, 383 K	4×10^{10}	16
1 atm, 298 ± 1 K, 0.5−10 ppm Hg, 10−50 ppm Br_2	$(5.4 \pm 0.2) \times 10^7$ (upper limit)	25
1 atm, 297 ± 1 K, 0.2 ppm Hg, 13 ppm Br_2	$(3.6 \pm 0.5) \times 10^7$	27
1 atm, 373 K, 0.16 ppm Hg, 10 ppm Br_2	2.62×10^7	29

Table 6. Rate Constants from Experimental Conversion of Hg (Hg + I_2) from the Literature

conditions	rate constant (cm^3 mol^{-1} s^{-1})	ref
	$Hg + I_2 \leftrightarrow HgI_2$	
1 atm, 296 ± 2 K, ∼0.5 ppm Hg, 130 ppm I_2	$(7.6 \pm 0.3) \times 10^4$ (upper limit)	26
1 atm, 373 K, 0.16 ppm Hg, 5.1 ppm I_2	1.20×10^8	30

procedure, and developed the B97 method. B97-1 was a modification by Hamprecht et al. and showed that the geometries calculated, including the geometries of a set of transition metal compounds, were improved over the BLYP functional.[49] More recently, Chai and Head-Gordon proposed a new long-range corrected (LC) hybrid functional, ωB97X, which includes the short-range (SR) Hartree−Fock (HF) exchange.[50] B2PLYP is based on a mixing of standard generalized gradient approximations (GGAs) for exchange by Becke (B) and for correlation by Lee, Yang, and Parr (LYP) with HF exchange and a perturbative second-order correlation part (PT2) that is obtained from the Kohn−Sham (GGA) orbitals and eigenvalues.[51] In 2008 Zhao and Truhlar presented two new hybrid meta exchange correlation functionals, called M06 and M06-2X. The M06 functional is parametrized for both transition metals and nonmetals, whereas the M06-2X functional is a high nonlocality functional with double the amount of nonlocal exchange (2X), and it is parametrized only for nonmetals.[52] CCSD(T)[53−56] is a coupled-cluster method that includes singles and doubles fully, and triples are calculated noniteratively.[57]

Three different basis sets were used, LANL2DZ (Los Alamos National Laboratory 2 double-ζ), SDD (Stuttgart−Dresden double-ζ), and aug-cc-pVTZ[58,59] (augmented correlation consistent basis sets of triple-ζ quality). For the latest, scalar relativistic effects were employed through the use of small-core relativistic pseudopotentials (PP)[60] for the 60 and 10 inner electrons of Hg and Br, respectively. The LANL2DZ basis set includes the Los Alamos National Laboratories double-ζ effective core potential (ECP) for the sodium through bismuth elements, which was developed by Hay and Wadt.[61] The SDD basis set includes a Stuttgart−Dresden ECP for the remainder of the elements after the first row.[62−64] All calculations were performed as implemented in the Gaussian 03[65] and Gaussian 09[66] suites.

Rate Constants. Association, insertion, and addition reactions have been treated as chemical activation reactions with quantum Rice Ramsperger Kassel (qRRK) analysis for $k(E)$ and master equation (ME) analysis for falloff (pressure/temperature dependent stabilization of the energized adduct).[42] Unimolecular dissociation reactions are also treated with qRRK $k(E)$/ME analysis. Kinetics of these small molecules (several atom species,

Table 7. Elementary Rate Constants from the Literature for Reactions of Hg and HgCl with Chlorine

reacn	A (cm^3 mol^{-1} s^{-1})	n	Ea (kcal mol^{-1})	ref
$Hg + Cl \leftrightarrow HgCl$	2.4×10^8	1.4	−14400	44
	1.95×10^{13}	0.0	0	23
$HgCl + Cl_2 \leftrightarrow HgCl_2 + Cl$	1.39×10^{14}	0.0	1000	44
$Hg + Cl_2 \leftrightarrow HgCl + Cl$	1.39×10^{14}	0.0	34000	42
	6.15×10^{13}	0.0	43300	33
$HgCl + Cl \leftrightarrow HgCl_2$	2.19×10^{18}	0.0	3100	44
	1.95×10^{13}	0.0	0	23

Table 8. Elementary Rate Constants from the Literature for Reactions of Hg and HgBr with Bromine

reacn	A (cm^3 mol^{-1} s^{-1})	n	Ea (kcal mol^{-1})	ref
$Hg + Br \leftrightarrow HgBr$	6.63×10^{11}	0.0	0	12
	2.75×10^{11}	0.0	−1620	33
$HgBr + Br_2 \leftrightarrow HgBr_2 + Br$	1.11×10^{14}	0	60	39
$Hg + Br_2 \leftrightarrow HgBr + Br$	1.15×10^{15}	0.0	30100	33
$HgBr + Br \leftrightarrow HgBr_2$	1.51×10^{14}	0.0	0	12

dx.doi.org/10.1021/jp412654s | J. Phys. Chem. A XXXX, XXX, XXX−XXX

Table 9. Elementary Rate Constants from the Literature for Reactions of Hg with Iodine

reacn	A (cm^3 mol^{-1} s^{-1})	n	Ea (kcal mol^{-1})	ref
Hg + I ↔ HgI	2.41×10^{11}	−2.38	0.0	12

examples HgCl, $HgCl_2$, and so on) are in the low pressure or falloff kinetic regions and show a temperature and pressure dependence in the kinetics. Input rate expressions for the qRRK analysis are from the works of the Peterson,[8] Goodsite[12] and Wilcox[33,35] groups and this study.

The chemical activation kinetics for Hg + X_2 → HgX_2 insertion reactions have been estimated from the theoretical calculations in this study. We exercise the model by varying these rate constants to illustrate the significant differences in barrier that are needed from the calculated values to try and match experimental data. Temperature and pressure dependence of the rate constants were calculated with the Chemaster Code.[67] The Supporting Information (Table S3) summarizes the parameters used for the determination of the qRRK $k(E)$/ME analysis and the figures with the pressure and temperature dependence of the rate constants. The rate constant for the reaction

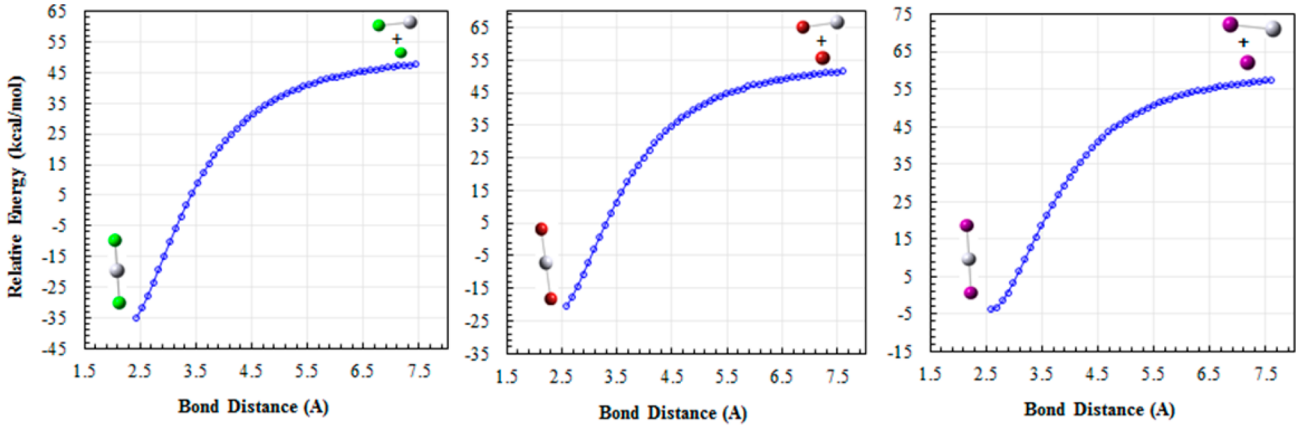

Figure 1. Potential energy diagrams for the ClHg···Cl (left), BrHg···Br (middle), and IHg···I (right) bonds.

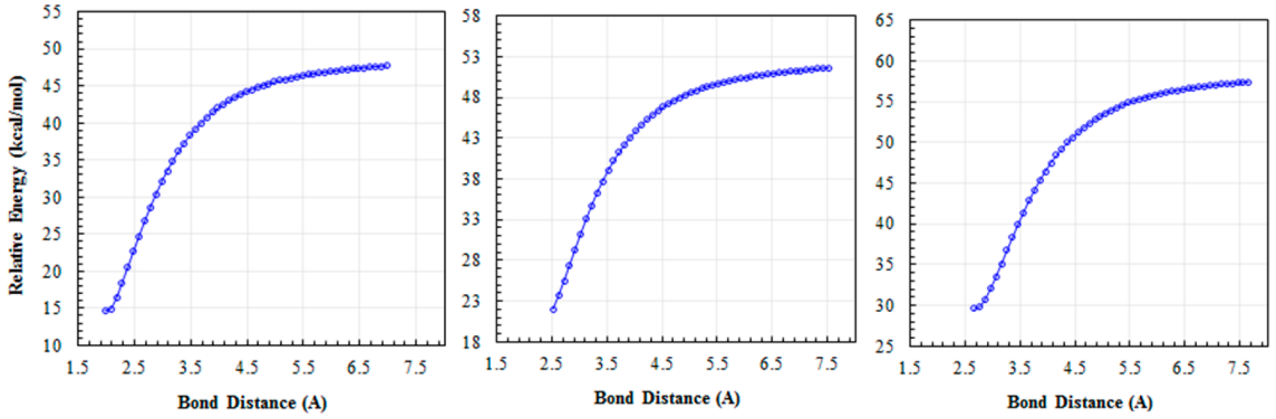

Figure 2. Potential energy diagrams for the HgCl···Cl (left), HgBr···Br (middle), and HgI···I (right) bonds.

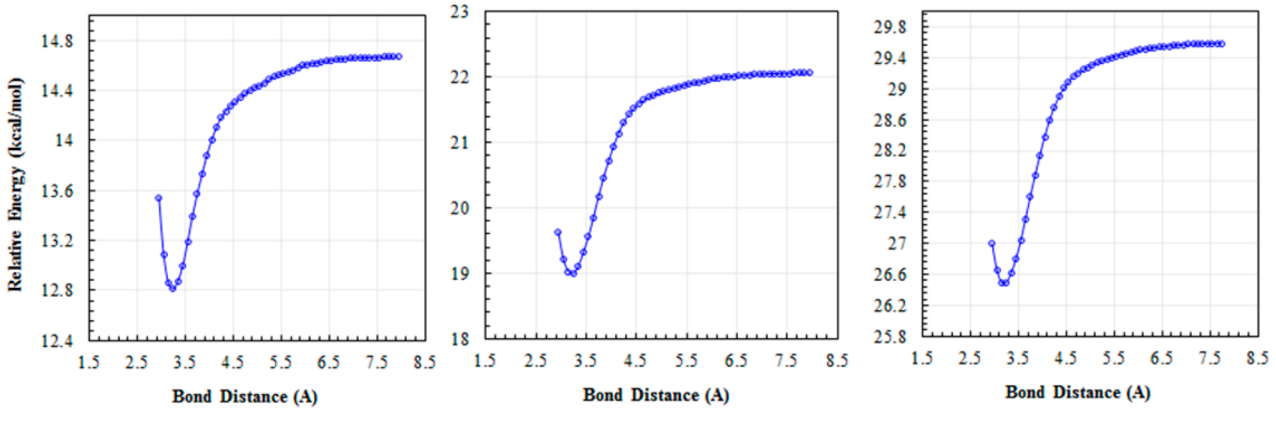

Figure 3. Potential energy diagrams for the Hg···ClCl (left), Hg···BrBr (middle), and Hg···II (right) bonds.

dx.doi.org/10.1021/jp412654s | J. Phys. Chem. A XXXX, XXX, XXX−XXX

Table 10. Reaction Mechanism from the Literature for the Conversion of Hg by Chlorine

reacn	A (cm^3 mol^{-1} s^{-1})	n	Ea (cal mol^{-1})	ref
$Cl + Cl \leftrightarrow Cl_2$	5.79×10^{14}	0.0	−1600	70
$Hg + Cl \leftrightarrow HgCl$	2.4×10^{8}	1.4	−14400	44
$HgCl + Cl_2 \leftrightarrow HgCl_2 + Cl$	1.39×10^{14}	0.0	1000	44
$Hg + Cl_2 \leftrightarrow HgCl + Cl$	6.15×10^{13}	0.0	43300	33
$HgCl + Cl \leftrightarrow HgCl_2$	2.19×10^{18}	0.0	3100	44

Table 11. Reaction Mechanism from the Literature for the Conversion of Hg by Bromine

reacn	A (cm^3 mol^{-1} s^{-1})	n	Ea (cal mol^{-1})	ref
$Br + Br \leftrightarrow Br_2$	1.48×10^{14}	0	−1700	71
$Hg + Br \leftrightarrow HgBr$	2.75×10^{11}	0.0	−1620	33
$HgBr + Br_2 \leftrightarrow HgBr_2 + Br$	1.11×10^{14}	0	60	39
$Hg + Br_2 \leftrightarrow HgBr + Br$	1.15×10^{15}	0.0	30100	33
$HgBr + Br \leftrightarrow HgBr_2$	1.51×10^{14}	0.0	0	12

Table 12. Reaction Mechanism from the Literature for the Conversion of Hg by Iodine

reacn	A (cm^3 mol^{-1} s^{-1})	n	Ea (cal mol^{-1})	ref
$I + I \leftrightarrow I_2$	2.00×10^{14}	0.0	−1143	72
$Hg + I \leftrightarrow HgI$	1.86×10^{17}	−2.38	0.0	12
$HgI + I_2 \leftrightarrow HgI_2 + I$	1.48×10^{16}	0.0	0.0	*a*
$Hg + I_2 \leftrightarrow Hg\,I + I$	8.68×10^{18}	0.0	27796	*a*
$HgI + I \leftrightarrow HgI_2$	3.66×10^{10}	0.0	0.0	*a*

[a]This work.

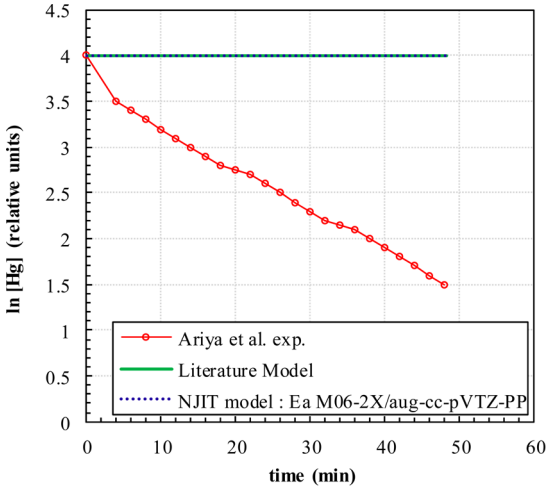

Figure 4. Hg loss by reaction with Cl_2 (1 ppm Hg, 10 ppm Cl_2 at 298 K and 1 atm): (a) red circles, Ariya et al.'s[25] experimental data; (b) solid green line, kinetics from elementary reaction mechanism from the literature; (c) dotted blue line, kinetics from elementary reaction mechanism from NJIT (the literature model and the NJIT model overlap).

$HgBr_2 \rightarrow Hg + Br_2$ was calculated by ChemRate in order to check the consistency of the Chemaster calculations. ChemRate contains a master equation solver so that rate constants for unimolecular reactions in the energy transfer region and chemical activation processes under steady and nonsteady state conditions can be determined on the basis of Rice Ramsperger Kassel Marcus (RRKM) theory.[68,69] Results show good agreement between the results obtained by ChemRate and Chemaster. The Supporting Information (Figure S4) contains the comparison.

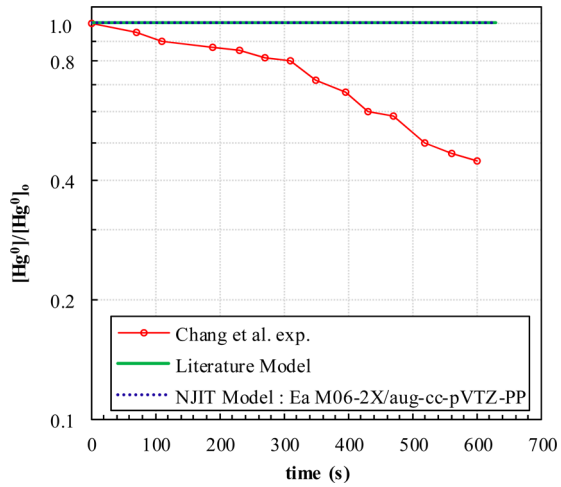

Figure 5. Hg loss by reaction with Cl_2 (0.2 ppm Hg, 242 ppm Cl_2 at 297 K and 1 atm): (a) red circles, Chang et al.'s[28] experimental data; (b) solid green line, kinetics from elementary reaction mechanism from the literature; (c) dotted blue line, kinetics from elementary reaction mechanism from NJIT (the literature model and the NJIT model overlap).

Solution (Numerical Integration) of the Elementary Kinetic Mechanism (Chemkin). The Chemkin Code V3.2[24] was used to set up and solve the differential equations for the mechanisms we have used. Enthalpies of formation, entropies, and heat capacities from the literature or calculated in this work for the species involved in the mechanism are reported in the Supporting Information (Table S1). Reverse reaction rate constants are determined from the thermochemistry and the forward rate constant (reactions are thermodynamically consistent).

RESULTS AND DISCUSSION

The reactions considered for the oxidation of Hg by chlorine, bromine, and iodine are (where X = Cl, Br, I):

$$Hg + X \rightarrow HgX$$

(exothermic by 24.9, 13.5, and 8.3 kcal mol^{-1} for Cl, Br, and I, but need an atom source)

dx.doi.org/10.1021/jp412654s | J. Phys. Chem. A XXXX, XXX, XXX−XXX

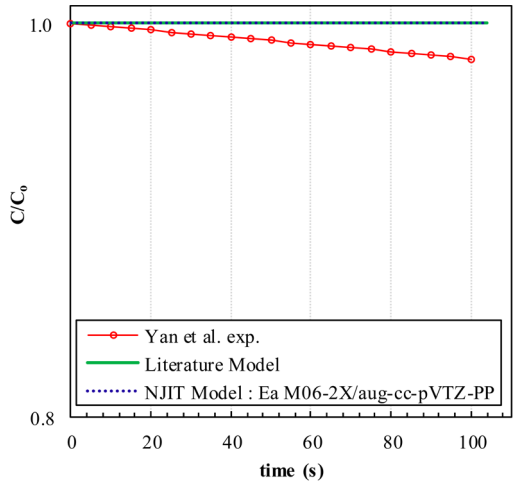

Figure 6. Hg loss by reaction with Cl_2 (0.16 ppm Hg, 10 ppm Cl_2 at 373 K and 1 atm): (a) red circles, Yan et al.'s[29] experimental data; (b) solid green line, kinetics from elementary reaction mechanism from the literature; (c) dotted blue line, kinetics from elementary reaction mechanism from NJIT (the literature model and the NJIT model overlap).

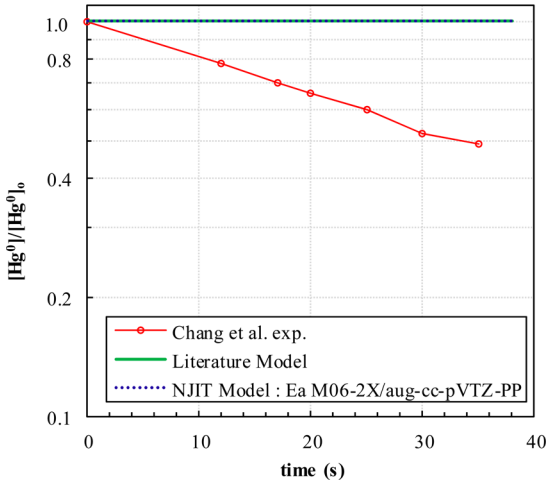

Figure 7. Hg loss by reaction with Br_2 (0.2 ppm Hg, 13 ppm Br_2 at 296 K and 1 atm): (a) red circles, Chang et al.'s[27] experimental data; (b) solid green line, kinetics from elementary reaction mechanism from the literature; (c) dotted blue line, kinetics from elementary reaction mechanism from NJIT (the literature model and the NJIT model overlap).

$$HgX + X \rightarrow HgX_2$$

(exothermic by 82.7, 72.0, and 61.3 kcal mol^{-1} for Cl, Br, and I, but need an atom source)

$$HgX + X_2 \rightarrow HgX_2 + X$$

(exothermic by 24.2, 25.9, and 25.2 kcal mol^{-1} for Cl, Br, and I, but need an atom source to form HgX)

$$Hg + X_2 \rightarrow HgX + X$$

(exothermic by 33.1, 29.6, and 27.8 kcal mol^{-1} for Cl, Br, and I, plus have barriers of 43.3, 30.1, 27.7 kcal mol^{-1} for Cl, Br, and I)

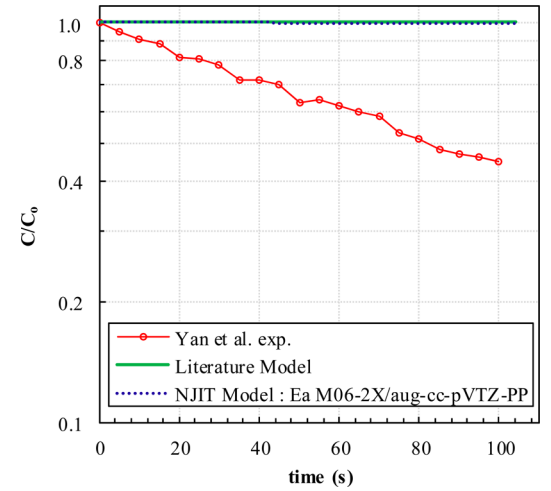

Figure 8. Hg loss by reaction with Br_2 (0.16 ppm Hg, 10 ppm Br_2 at 373 K and 1 atm): (a) red circles, Yan et al.'s[29] experimental data; (b) solid green line, kinetics from elementary reaction mechanism from the literature; (c) dotted blue line, kinetics from elementary reaction mechanism from NJIT (the literature model and the NJIT model overlap).

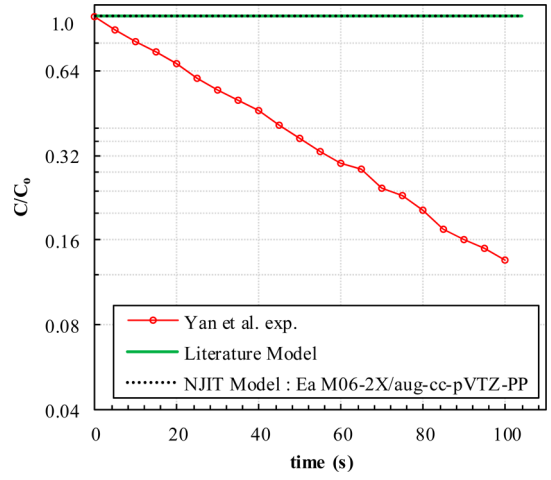

Figure 9. Hg loss by reaction with I_2 (160 ppb_v Hg, 5.1 ppm I_2 at 373 K and 1 atm): (a) red circles, Yan et al.'s[30] experimental data; (b) solid green line, kinetics from elementary reaction mechanism from the literature; (c) dotted blue line, kinetics from elementary reaction mechanism from NJIT (the literature model and the NJIT model overlap).

Ariya et al. (2002)[25,26] used a tubular flow reactor to study the oxidation of mercury by chlorine, bromine, and iodine at atmospheric conditions (1 atm, 298 K). They followed the loss of mercury for reaction under conditions of different halogen concentrations. Chang et al.[27,28] also reported experimental results on the low temperature oxidation of mercury (1 atm, 296 K) by both chlorine and bromine, with data obtained by measuring the concentration of Hg° as a function of time in Pyrex flasks by mercury cold vapor atomic absorption spectrophotometry with a vacuum system for gas handling. Yan et al.[29,30] published experimental data on the oxidation of mercury by chlorine, bromine, iodine, BrCl, and ICl at 1 atm and 373 K, by in situ monitoring of the concentration of Hg° in the reactor (a stainless steel cylinder) as a function of time, monitoring mercury by cold vapor atomic adsorption spectrophotometer. These experiments did not have any planned atom sources to

dx.doi.org/10.1021/jp412654s | J. Phys. Chem. A XXXX, XXX, XXX−XXX

Table 13. Calculated Frequencies (cm^{-1}) for Chlorine Species and Comparison to Available Literature Data

		level of theory						
species	ref	B3LYP/ LanL2DZ	B3LYP/ SDD	B3LYP/ aug-cc-pVTZ-PP	ωB97X/ aug-cc-pVTZ-PP	B2PLYP/ aug-cc-pVTZ-PP	M06/ aug-cc-pVTZ-PP	M06-2X/ aug-cc-pVTZ-PP
$HgCl_2$	*100*[a]	68	83	98	103	102	99	98
	313[b], *366*[c]	290	314	338	362	353	352	344
	376[c], *413*[d]	347	379	392	411	407	404	392
Cl_2	*559.71*[e]	468	471	539	597	552	573	576
TS ClHgCl (sym)				−212	−326	−242	−237	−314
				121	148	124	140	139
				198	159	233	185	214
TS ClHgCl (nonsym)		−162	−210	−262	−396	−160	−277	−349
		99	110	107	133	121	117	127
		238	236	223	246	243	226	245

[a]Reference 73. [b]Reference 74. [c]Reference 75. [d]Reference 76. [e]Reference 77.

Table 14. Calculated Bond Lengths (Å) and Bond Angles (deg) for Chlorine Species and Comparison to Available Literature Data

			level of theory						
species	bond length/ bond angle	ref	B3LYP/ LanL2DZ	B3LYP/ SDD	B3LYP/ aug-cc-pVTZ-PP	ωB97X/ aug-cc-pVTZ-PP	B2PLYP/ aug-cc-pVTZ-PP	M06/ aug-cc-pVTZ-PP	M06-2X/ aug-cc-pVTZ-PP
$HgCl_2$	*r*(ClHg)	*2.25*[a], *2.44*[b]	2.44	2.37	2.29	2.26	2.27	2.28	2.28
	θ(ClHgCl)	*180*[a]	180.00	180.00	180.00	180.00	180.00	180.00	180.00
Cl_2	*r*(ClCl)	*1.99*[c]	2.22	2.23	2.02	1.96	2.01	2.00	2.00
TS ClHgCl (sym)	*r*(ClHg)				2.79	2.79	2.67	2.78	2.74
	r(HgCl)				2.79	2.79	2.67	2.78	2.74
	θ(ClHgCl)				55.53	54.65	56.74	55.47	55.56
TS ClHgCl (nonsym)	*r*(ClHg)		3.01	2.83	2.76	2.71	2.65	2.73	2.73
	r(HgCl)		2.85	2.80	2.70	2.65	2.64	2.69	2.66
	θ(ClHgCl)		53.78	57.76	54.87	56.87	61.14	57.31	57.25

[a]Reference 78. [b]Reference 79. [c]Reference 77.

Table 15. Calculated Frequencies (cm^{-1}) for Bromine Species and Comparison to Available Literature Data

		level of theory						
species	ref	B3LYP/ LanL2DZ	B3LYP/ SDD	B3LYP/ aug-cc-pVTZ-PP	ωB97X/ aug-cc-pVTZ-PP	B2PLYP/ aug-cc-pVTZ-PP	M06/ aug-cc-pVTZ-PP	M06-2X/ aug-cc-pVTZ-PP
$HgBr_2$	*68*[a], *71.6*[b]	46	59	65	69	68	65	66
	222[c], *229*[d], *226.9*[b]	179	200	207	225	218	212	212
	297.8[e], *302.5*[b]	244	272	276	295	288	282	275
Br_2	*325.3*[f]	270	281	317	347	326	331	345
TS BrHgBr (sym)	*−189.4*[g]			−128	−172	−149	−130	−184
	55.7[g]			88	79	100	106	106
	152.6[g]			134	123	150	115	125
TS BrHgBr (nonsym)		−122	−149	−178	−273	−148	−189	−222
		71	69	80	96	102	84	94
		146	143	149	169	162	149	167

[a]Reference 80. [b]Reference 8. [c]Reference 81. [d]Reference 82. [e]Reference 46. [f]Reference 83. [g]Reference 8.

initiate the reaction. Loss of Hg and/or HgX_2 formation is observed in these three sets of experiments, and rate constants for the reaction of Hg with X_2 to form HgX_2 are reported.

One possible source for formation of HgX_2 is an insertion reaction (the reactions Hg + X_2 → HgX + X and dissociation of X_2 → X + X are sufficiently endothermic to limit their consideration). Table 3 summarizes the theoretically calculated barriers and rate constants reported in the literature for the insertion reaction (Hg + X_2 → HgX_2, Ea = 39.5 and 27.2 kcal mol^{-1} for chlorine and bromine, respectively).

Tables 4−6 present a summary of the reported experimental data on rate constants for the reactions of mercury with molecular chlorine, bromine, and iodine, respectively (Hg + X_2 → HgX_2). Tables 7−9 summarize the rate constants available in the literature for the oxidation of mercury by chlorine, bromine, and iodine, respectively. The reactions between Hg and the molecular halogens are

$$Hg + X_2 \rightarrow HgX_2 \quad (1)$$

dx.doi.org/10.1021/jp412654s | J. Phys. Chem. A XXXX, XXX, XXX−XXX

Table 16. Calculated Bond Lengths (Å) and Bond Angles (deg) for Bromine Species and Comparison to Available Literature Data

			level of theory						
species	bond length/ bond angle	ref	B3LYP/ LanL2DZ	B3LYP/SDD	B3LYP/ aug-cc-pVTZ-PP	ωB97X/ aug-cc-pVTZ-PP	B2PLYP/ aug-cc-pVTZ-PP	M06/ aug-cc-pVTZ-PP	M06-2X/ aug-cc-pVTZ-PP
$HgBr_2$	r(BrHg)	2.404[a], 2.37[b]	2.58	2.48	2.42	2.39	2.40	2.42	2.41
	θ(BrHgBr)	180[a]	179.40	179.46	180.00	180.00	180.00	180.00	180.00
Br_2	r(BrBr)	2.28[c], 2.288[a]	2.51	2.45	2.32	2.28	2.30	2.29	2.28
TS BrHgBr (sym)	r(BrHg)	2.85[a]			2.90	2.98	2.80	2.94	2.88
	r(HgBr)	2.85[a]			2.90	2.98	2.80	2.94	2.88
	θ(BrHgBr)	55.74[a]			60.47	58.64	61.27	60.21	59.57
TS BrHgBr (nonsym)	r(BrHg)		3.03	2.96	2.88	2.81	2.80	2.84	2.84
	r(HgBr)		3.08	2.92	2.80	2.75	2.75	2.80	2.80
	θ(BrHgBr)		58.86	61.66	62.54	64.48	65.62	62.85	62.84

[a]Reference 8. [b]Reference 84. [c]Reference 80.

Table 17. Calculated Frequencies (cm^{-1}) for Iodine Species and Comparison to Available Literature Data

		level of theory						
species	ref	B3LYP/ LanL2DZ	B3LYP/SDD	B3LYP/ aug-cc-pVTZ-PP	ωB97X/ aug-cc-pVTZ-PP	B2PLYP/ aug-cc-pVTZ-PP	M06/ aug-cc-pVTZ-PP	M06-2X/ aug-cc-pVTZ-PP
HgI_2	51[c], 53.7[i], 63[d]	68	47	49	52	52	50	49
	155[e], 156[c], 158[f], 163.7[i]	290	143	148	161	156	150	152
	235[c], 237.5[g], 240.5[i]	346	220	220	236	230	224	221
I_2	214.5[a], 218.1[b,i]	468	185	212	233	219	218	234
TS IHgI (nonsym)		−162	−121	−146	−242	−55	−151	−183
		99	62	70	83	19	77	81
		238	107	112	128	30	113	128

[a]Reference 85. [b]Reference 86. [c]Reference 87. [d]Reference 88. [e]Reference 89. [f]Reference 81. [g]Reference 90. [h]Reference 91. [i]Reference 32.

Table 18. Calculated Bond Lengths (Å) for Iodine Species and Comparison to Available Literature Data

			level of theory						
species	bond length/ bond angle	ref	B3LYP/ LanL2DZ	B3LYP/SDD	B3LYP/ aug-cc-pVTZ-PP	ωB97X/ aug-cc-pVTZ-PP	B2PLYP/ aug-cc-pVTZ-PP	M06/ aug-cc-pVTZ-PP	M06-2X/ aug-cc-pVTZ-PP
HgI_2	r(IHg)	2.5[d,e]	2.44	2.66	2.61	2.58	2.59	2.62	2.59
	θ(IHgI)	180.0[b]	180.00	180.00	180.00	180.00	180.00	180.00	180.00
I_2	r(II)	2.66[a,b,e], 2.67[c]	2.22	2.85	2.70	2.66	2.69	2.69	2.66
TS IHgI (nonsym)	r(IHg)		3.26	3.19	3.09	3.01	4.11	3.03	3.06
	r(HgI)		3.20	3.05	2.94	2.89	4.10	2.95	2.87
	θ(IHgI)		63.95	67.28	68.43	67.51	73.60	69.04	67.17

[a]Reference 85. [b]Reference 86. [c]Reference 32. [d]Reference 87. [e]Reference 32.

$$Hg + X_2 \rightarrow HgX + X \quad (2)$$

The bond dissociation reactions XHg—X, HgX—X, and Hg—XX (*X* = Cl, Br, I) are barrierless (as indicated in Figures 1−3), and several rate constants for reaction 2 have been reported in the literature.[8,33,35] At atmospheric conditions, the endothermic reaction $Hg + X_2 \rightarrow HgX + X$ is not important and will not result in loss of Hg. Therefore, the only possible reaction at atmospheric conditions is $Hg + X_2 \rightarrow HgX_2$.

We modeled the data from the several sets of experiments performed by Ariya et al.,[25,26] Chang et al.,[27,28] and Yan et al.[29,30] for chlorine, bromine, and iodine. For the modeling, we used detailed reaction mechanisms with reactions that follow fundamental thermodynamics and microscopic reversibility, where the rate constants were taken from the literature. The mechanisms used for the modeling with the literature experimental data are summarized in Tables 10−12. Figures 4−9 represent the comparison between the experimental data and the model results using the available rate constants in the literature. In Figures 4−9, (a) red circles are experimental data, (b) solid green lines are kinetics from the elementary reaction mechanism from the literature, and (c) dashed blue lines represent kinetics from elementary reaction mechanism from New Jersey Institute of Technology (NJIT; the literature model and the NJIT model overlap). In trying to reproduce the experimental results with the rate constants and submechanisms

dx.doi.org/10.1021/jp412654s | J. Phys. Chem. A XXXX, XXX, XXX−XXX

Table 19. Reaction Enthalpies and Energies of Activation for $Hg + Cl_2 \rightarrow HgCl_2$[a]

		level of theory							
param	ref	B3LYP/ LanL2DZ	B3LYP/SDD	B3LYP/ aug-cc-pVTZ-PP	ωB97X/ aug-cc-pVTZ-PP	B2PLYP/ aug-cc-pVTZ-PP	M06/ aug-cc-pVTZ-PP	M06-2X/ aug-cc-pVTZ-PP	CCSD(T)/ aug-cc-pVTZ-PP
					$Hg + Cl_2 \rightarrow HgCl_2$				
ΔH_{rxn}	*−49.63*[b]	−54.96	−51.71	−44.18	−55.34	−46.82	−47.21	−49.10	−47.93
$\Delta H_{calc} - \Delta H_{expt}$		*5.33*	*2.08*	*5.45*	*5.71*	*2.81*	*2.42*	*0.53*	*1.70*
Ea (sym TS)	*39.49*[c]	–	–	29.95	30.18	35.18	32.38	39.01	
Ea (nonsym TS)		13.81	14.89	37.33	44.22	38.28	37.90	45.07	

[a]Units: kcal mol^{-1}. [b]Reference 92. [c]Reference 36.

Table 20. Reaction Enthalpies and Energies of Activation for $Hg + Br_2 \rightarrow HgBr_2$[a]

		level of theory							
param	ref	B3LYP/ LanL2DZ	B3LYP/SDD	B3LYP/ aug-cc-pVTZ-PP	ωB97X/ aug-cc-pVTZ-PP	B2PLYP/ aug-cc-pVTZ-PP	M06/ aug-cc-pVTZ-PP	M06-2X/ aug-cc-pVTZ-PP	CCSD(T)/ aug-cc-pVTZ-PP
					$Hg + Br_2 \rightarrow HgBr_2$				
ΔH_{rxn}	*−42.48*[b]	−42.87	−41.41	−35.98	−46.11	−39.31	−34.56	−42.51	−41.86
$\Delta H_{calc} - \Delta H_{expt}$		*0.39*	*1.07*	*6.5*	*3.63*	*3.17*	*7.92*	*0.03*	*0.62*
Ea (sym TS)	*27.2*[c]	–	–	25.66	35.61	30.28	24.27	33.18	
Ea (nonsym TS)		15.19	24.81	33.35	46.38	34.98	33.03	**39.89**	

[a]Units: kcal mol^{-1}. [b]Reference 92. [c]Reference 8..

dx.doi.org/10.1021/jp412654s | J. Phys. Chem. A XXXX, XXX, XXX−XXX

Table 21. Reaction Enthalpies and Energies of Activation for Hg + I_2 → HgI_2[a]

		level of theory							
param	ref	B3LYP/ LanL2DZ	B3LYP/SDD	B3LYP/ aug-cc-pVTZ-PP	ωB97X/ aug-cc-pVTZ-PP	B2PLYP/ aug-cc-pVTZ-PP	M06/ aug-cc-pVTZ-PP	M06-2X/ aug-cc-pVTZ-PP	CCSD(T)/ aug-cc-pVTZ-PP
				Hg + I_2 → HgI_2					
ΔH_{rxn}	−33.45[b]	−34.58	−34.41	−26.65	−36.17	−30.15	−25.28	−32.78	−32.96
$\Delta H_{calc} - \Delta H_{expt}$		*-1.14*	*-0.96*	*6.80*	*-2.72*	*3.30*	*8.17*	*0.66*	*0.49*
Ea (nonsymm TS)		18.13	24.81	31.48	42.89	57.20	28.90	**37.37**	

[a]Units: kcal mol^{-1}. [b]Reference 47.

Table 22. High Pressure Limit Rate Constants for the Insertion Reactions

reacn	A (cm^3 mol^{-1} s^{-1})	n	α	Ea (cal mol^{-1})
Hg + Cl_2 → $HgCl_2$	1.66×10^{10}	1.20	0	45513
Hg + Br_2 → $HgBr_2$	2.83×10^{10}	1.06	0	40438
Hg + I_2 → HgI_2	2.37×10^{10}	1.06	0	38020

Table 23. Rate Constants for the Insertion Reactions from 0.01 to 100 atm

reacn condition	A (cm^3 mol^{-1} s^{-1})	n	α	Ea (cal mol^{-1})
	Hg + Cl_2 → $HgCl_2$			
0.01 atm	4.14×10^{21}	−3.64	0	46746
0.1 atm	9.14×10^{22}	−3.74	0	47108
1 atm	1.44×10^{24}	−3.78	0	47953
10 atm	6.34×10^{23}	−3.39	0	48604
100 atm	9.00×10^{20}	−2.30	0	48384
	Hg + Br_2 → $HgBr_2$			
0.01 atm	7.03×10^{18}	−3.01	0	41861
0.1 atm	7.07×10^{19}	−3.01	0	41877
1 atm	7.03×10^{20}	−3.01	0	42005
10 atm	2.69×10^{21}	−2.89	0	42424
100 atm	3.44×10^{20}	−2.36	0	42744
	Hg + I_2 → HgI_2			
0.01 atm	2.55×10^{19}	−3.02	0	39389
0.1 atm	2.71×10^{20}	−3.03	0	39466
1 atm	2.33×10^{21}	−3.01	0	39835
10 atm	1.68×10^{21}	−2.68	0	40328
100 atm	8.33×10^{18}	−1.76	0	40224

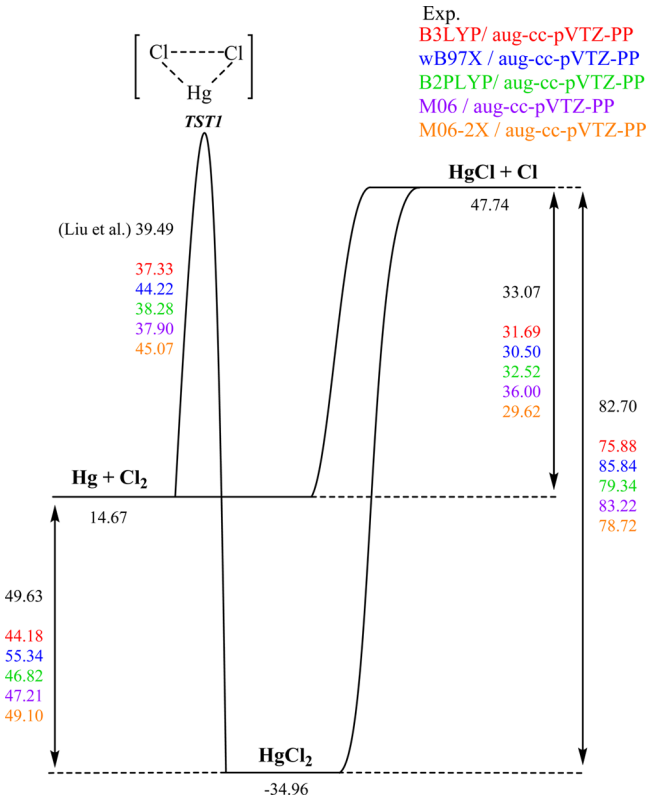

Figure 10. Potential energy diagram for the reaction Hg + Cl_2.

dx.doi.org/10.1021/jp412654s | J. Phys. Chem. A XXXX, XXX, XXX−XXX

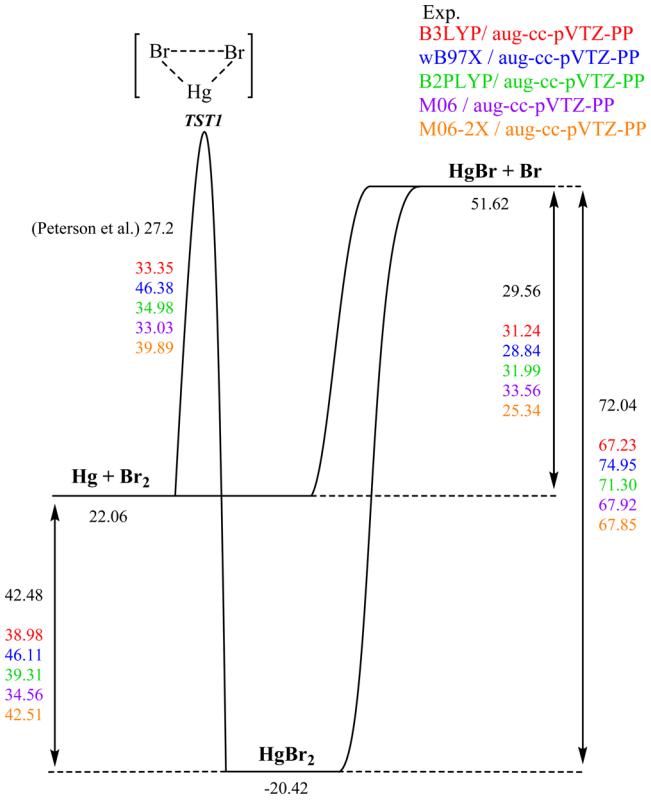

Figure 11. Potential energy diagram for insertion of Hg + Br_2.

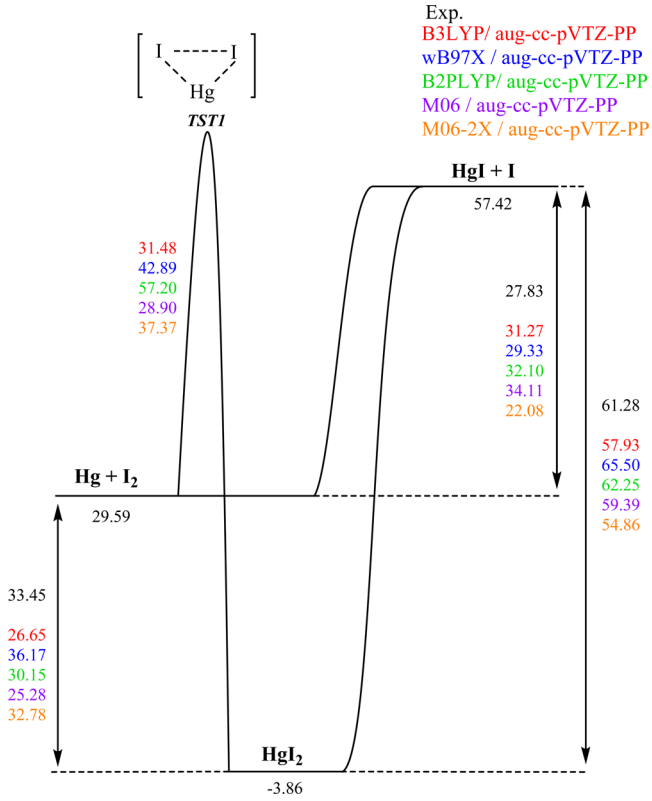

Figure 12. Potential energy diagram for the reaction Hg + I_2.

proposed in the literature (summarized in Table 10 for Cl_2, Table 11 for Br_2, and Table 12 for I_2), we find that, without an atom source, effectively no conversion of mercury and no agreement with the experimental data is obtained under atmospheric conditions. Our computational results indicate that experimental results cannot be explained by the mechanisms built by using the rate constants in the literature with thermodynamically consistent reactions.

Insertion Reaction Kinetics. In order to explain the experimentally observed mercury loss, we further studied the insertion reaction ($Hg + X_2 \rightarrow HgX_2$), and we evaluated (modeled) the influence of a source of halogen atoms in the reaction systems. The insertion reactions of mercury into chlorine, bromine, and iodine molecules forming HgX_2 are overall exothermic and serve as a possible option to reproduce (explain) the experimental results.

Using computational chemistry, we found an optimized, nonlinear, nonsymmetric Cl—Hg—Cl transition state structure, that can react directly to $HgCl_2$. The chemically activated $HgCl_2$* formed from this insertion can also undergo dissociation to HgCl + Cl. A similar complex and reaction system was also obtained for bromine and iodine, where $HgBr_2$ and HgI_2 are formed through a nonlinear X—Hg—X intermediate (X = Br, I). Two different transition states were found for the insertion reaction of mercury into chlorine and bromine: (i) symmetric and (ii) nonsymmetric. The symmetric transition states are found to have a lower barrier than the nonsymmetric transition states. However, in order to obtain the symmetric transition states, the symmetry of the two X—Hg—X bond lengths needed to be forced (frozen). Only the nonsymmetric was found for the insertion reaction of mercury into iodine. The nonsymmetric transition states are optimized structures and were used for the kinetic calculations.

Different levels of theory were used for the determination of the rate constants for comparison and for the selection of the most accurate method. Tables 13 and 14 summarize the geometries and frequencies obtained for the Hg—Cl system at the different levels of theory, Tables 15 and 16 represent the data for the Hg—Br system, and Tables 17 and 18 represent the data for the Hg—I system for the ground state and the transition state. Tables 19—21 represent the energetics (enthalpy of reaction and energy of activation) for each level of theory for Cl_2, Br_2, and I_2, respectively.

The M06-2X/aug-cc-pVTZ-PP calculation method shows excellent agreement with the experimental data, for the geometry, the frequencies, and enthalpies of reaction, for all chlorine, bromine, and iodine calculations. The M06-2X/aug-cc-pVTZ-PP level of theory was selected for the determination of the kinetics. Table 22 summarizes the high pressure rate constants calculated at the M06-2X/aug-cc-pVTZ-PP level of theory for the insertion reactions. Table 23 includes the rate constants at pressures from 0.01 to 100 atm for the mercury—chlorine/—bromine/—iodine systems, obtained from the master equation analysis. The barriers obtained at this level of theory are 45.1, 39.9, and 37.4 kcal mol^{-1} for chlorine, bromine, and iodine, respectively. The symmetric barriers obtained by our fixed geometry calculations are in good agreement with the available literature data: 39.49 (chlorine) and 27.2 kcal mol^{-1} (bromine), compared to our calculations, 39.01 (chlorine) and 33.18 kcal mol^{-1} (bromine), respectively.[8,36]

Figure 10 illustrates the potential energy diagram for the Hg + Cl_2 reaction system and includes a higher energy reaction for dissociation of the energized $HgCl_2$ complex into HgCl + Cl. Data in the figure include the energy of activation obtained at the different computational methods. Figures 11 and 12 illustrate the same for the bromine and iodine systems, respectively.

dx.doi.org/10.1021/jp412654s | J. Phys. Chem. A XXXX, XXX, XXX—XXX

Table 24. NJIT Reaction Mechanism for the Oxidation of Hg by Chlorine

reacn	A (cm^3 mol^{-1} s^{-1})	n	Ea (cal mol^{-1})	ref
$Cl + Cl \leftrightarrow Cl_2$	5.79×10^{14}	0.0	−1600	70
$Hg + Cl \leftrightarrow HgCl$	2.40×10^{8}	1.4	−14400	44
$HgCl + Cl_2 \leftrightarrow HgCl_2 + Cl$	1.39×10^{14}	0.0	1000	44
$Hg + Cl_2 \leftrightarrow HgCl + Cl$	6.15×10^{13}	0.0	43300	33
$HgCl + Cl \leftrightarrow HgCl_2$	2.19×10^{18}	0.0	3100	44
$Hg + Cl_2 \leftrightarrow HgCl_2$	1.66×10^{10}	1.20	45513	*a*

[a]Rate constant calculated with the TST obtained with M06-2X/aug-cc-pVTZ-PP.

Table 25. NJIT Reaction Mechanism for the Oxidation of Hg by Bromine

reacn	A (cm^3 mol^{-1} s^{-1})	n	Ea (cal mol^{-1})	ref
$Br + Br \leftrightarrow Br_2$	1.48×10^{14}	0	−1700	71
$Hg + Br \leftrightarrow HgBr$	2.75×10^{11}	0.0	−1620	33
$HgBr + Br_2 \leftrightarrow HgBr_2 + Br$	1.11×10^{14}	0	60	39
$Hg + Br_2 \leftrightarrow HgBr + Br$	1.15×10^{15}	0.0	30100	33
$HgBr + Br \leftrightarrow HgBr_2$	1.51×10^{14}	0.0	0	12
$Hg + Br_2 \leftrightarrow HgBr_2$	2.83×10^{10}	1.06	40438	*a*

[a]Rate constant calculated with the TST obtained with M06-2X/aug-cc-pVTZ-PP.

Table 26. NJIT Reaction Mechanism for the Oxidation of Hg by Iodine

reacn	A (cm^3 mol^{-1} s^{-1})	n	Ea (cal mol^{-1})	ref
$I + I + M \leftrightarrow I_2 + M$	2.00×10^{14}	0.0	−1143	72
$Hg + I \leftrightarrow HgI$	1.86×10^{17}	−2.38	0.0	12
$HgI + I_2 \leftrightarrow HgI_2 + I$	1.48×10^{16}	0.0	0.0	*a*
$Hg + I_2 \leftrightarrow HgI + I$	8.68×10^{18}	0.0	27796	*a*
$HgI + I \leftrightarrow HgI_2$	3.66×10^{10}	0.0	0.0	*a*
$Hg + I_2 \leftrightarrow HgI_2$	2.37×10^{10}	1.06	38020	*b*

[a]This work. [b]Rate constant calculated with the TST obtained with M06-2X/aug-cc-pVTZ-PP.

Table 27. Energies of Activation Needed To Fit the Experimental Data

reacn	Ea (kcal mol^{-1})	ref
$Hg + Cl_2 \rightarrow HgCl_2$	9.5	Ariya et al.[25,26]
	10.8	Chang et al.[27,28]
	12.1	Yan et al.[29,30]
	45.07	theoretical[a]
$Hg + Br_2 \rightarrow HgBr_2$	7.3	Ariya et al.[25,26]
	7.5	Chang et al.[27,28]
	9.8	Yan et al.[29,30]
	39.89	theoretical[a]
$Hg + I_2 \rightarrow HgI_2$	8.6	Yan et al.[29,30]
	37.37	theoretical[a]

[a]This work.

We return to the kinetic modeling to determine the influence of including the insertion reactions in the model (using the rate constants calculated in this study). The inclusion of the calculated transition state rate constants to the mechanism (Tables 24−26) does not result in any conversion of mercury, as illustrated in Figures 4−9.

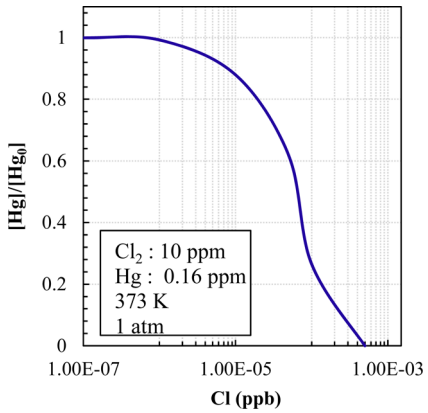

Figure 13. Conversion of Hg versus Cl atom concentration, with initially 0.16 ppm Hg and 10 ppm Cl_2 at 373 K and 1 atm.

The mercury conversion data reported in the literature are used to empirically calculate an energy barrier (Ea_{fit}) for the reaction $Hg + X_2 \rightarrow HgX_2$ that would explain the experiments.

$$k = AT^n \exp\left(\frac{-Ea}{RT}\right) \Rightarrow Ea_{fit} = -RT \ln\left(\frac{k_{exp}}{A_{th}T^{n_{th}}}\right)$$

where R is the universal gas constant, k_{exp} is the rate constant from the literature, A_{th} is the preexponential factor calculated at the M06-2X/aug-cc-pVTZ-PP level of theory, n_{th} is the temperature power calculated at the M06-2X/aug-cc-pVTZ-PP level of theory, and Ea_{fit} is the energy of activation that would be needed to fit the experimental rate constants, at the given temperature the experiments were performed.

The energy of activation obtained to fit Ariya et al.'s experimental rate constant for the reaction $Hg + Cl_2 \rightarrow HgCl_2$ is 9.5 kcal mol^{-1}, an Ea of 10.8 kcal mol^{-1} was needed to fit

Table 28. Conversion of Hg versus Cl Atom Concentration, with Initially 0.2 ppm Hg and 242 ppm Cl_2 at 297 K and 1 atm (Reaction Mechanism from Table 25)

Cl_2/Cl concn	10 ppm Cl_2/(0 ppb Cl)	10 ppm Cl_2/(1.0×10^{-6} ppb Cl)	10 ppm Cl_2/(1.0×10^{-5} ppb Cl)	10 ppm Cl_2/(1.0×10^{-4} ppb Cl)	10 ppm Cl_2/(1.0×10^{-3} ppb Cl)
$[Hg]/[Hg]_0$	1.0	0.993	0.879	0.264	0.0

dx.doi.org/10.1021/jp412654s | J. Phys. Chem. A XXXX, XXX, XXX−XXX

Table 29. Conversion of Hg versus Br Atom Concentration, with Initially 0.2 ppm Hg and 13ppm Br_2 at 296 K and 1 atm (Reaction Mechanism from Table 26)

Br_2/Br concn	10 ppm Br_2/(0 ppb Br)	10 ppm Br_2/(1.0×10^{-2} ppb Br)	10 ppm Br_2/(1.0×10^{-1} ppb Br)	10 ppm Br_2/(1.0×10^{-0} ppm Br)
$[Hg]/[Hg]_0$	1.0	0.921	0.449	0.0

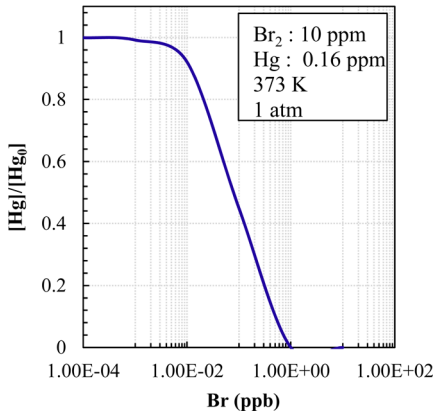

Figure 14. Conversion of Hg versus Br atom concentration, with initially 0.16 ppm Hg and 10 ppm Br_2 at 373 K and 1 atm.

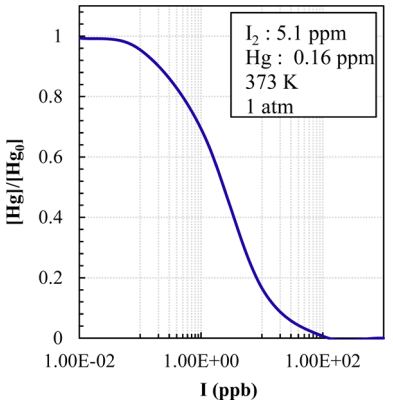

Figure 15. Conversion of Hg versus I atom concentration, with initially 0.16 ppm Hg and 5.1 ppm I_2 at 373 K and 1 atm.

Chang et.'s experimental rate constant, and an Ea of 12.1 kcal mol^{-1} was used to fit Yan et al.'s experimental rate constant.

The energy of activation calculated to fit Ariya et al.'s experimental rate constant for the reaction $Hg + Br_2 \rightarrow HgBr_2$ is 7.3 kcal mol^{-1}, an Ea of 7.5 kcal mol^{-1} was needed to fit Chang et al.'s experimental data, and an Ea of 9.8 kcal mol^{-1} was used to fit Yan et al.'s data.

The energy of activation determined to fit Yan et al.'s experimental rate constant for the reaction $Hg + I_2 \rightarrow HgI_2$ is 8.6 kcal mol^{-1}. Table 27 summarizes the results obtained for the energies of activation (the energies of activation needed to fit the experimental rate constants and the energies of activation calculated theoretically at the M06-2X/aug-cc-pVTZ level of theory). The energy of activation values obtained from the fits to the three experiments are similar for chlorine, bromine, and iodine. The empirical fit values are, however, on the order of 30 kcal mol^{-1} lower than the barriers calculated theoretically (45.1, 39.9, and 37.4 kcal mol^{-1} for chlorine, bromine, and iodine, respectively) and also similarly lower than the values calculated by other researchers with high or higher level calculation methods.

We do not feel it is justified to use the empirically calculated values in an insertion reaction to explain the atmospheric mercury conversion. We recommend the rate constants calculated at the M06-2X/aug-cc-pVTZ level of theory for the insertion reaction (summarized in Table 22).

Test of the Presence of Atomic Cl, Br, and I To Obtain a Model Fit to Mercury Conversion. Chang et al.'s experiments are carried out at room temperature, where they add Cl_2 to Hg in order to study the Hg loss. At room temperature, Cl_2 does not dissociate to Cl. However, in the experiments they use a continuous mercury light source to detect Hg atoms in a spherical bulb that could result in excited Hg* and reactions of Hg* with Cl_2 could result in dissociation of Cl_2 molecules to Cl atoms or insertion reaction. Their results also show that the use of a lower flux (pulsed) light source results in a significant decrease in Hg° loss relative to the continuous light source supporting a light or an Hg* interaction. Ariya et al. mention that in order to prevent the dissociation of I_2, the reaction is studied in a completely darkened chamber, and they also note the formation of particulate matter, which may infer heterogeneous reactions.

We performed a further modeling study to evaluate the possible effect of the presence of halogen atoms in the reaction systems as an initiation mechanism and to evaluate the concentration of atoms needed to explain the data. To test this case, we include the presence of Cl atoms in the reaction system for the Chemkin modeling, using the submechanism that includes the insertion reaction calculated at the M06-2X/aug-cc-pVTZ-PP level of theory. In the absence of Cl atoms, no conversion of Hg (initial concentration, 0.16 ppm) is observed. However, when Cl atoms are added, the conversion of Hg starts, and from the modeling results we conclude that $\sim 7.5 \times 10^{-5}$ ppb Cl would be necessary to obtain the ~45% conversion of mercury observed at Chang et al.'s experiments, and $\sim 10^{-3}$ ppb Cl atoms are necessary to obtain complete conversion of mercury, at the conditions of the experiment: 0.16 ppm Hg, 10 ppm Cl_2 at 373 K and 1 atm. Table 28 and Figure 13 illustrate the results of these calculations.

This modeling is also performed for bromine and iodine, to study the influence of atomic bromine and iodine in the reaction system. The bromine mechanism including the insertion reaction calculated at the M06-2X/aug-cc-pVTZ-PP level of theory has been used. Results indicate that higher concentrations of Br atoms are needed to affect conversion relative to chlorine.

Table 30. Conversion of Hg versus I Atom Concentration, with Initially 0.5 ppm Hg and 130 ppm I_2 at 296 K and 1 atm (Reaction Mechanism from Table 27)

I_2/I concn	10 ppm I_2/(0 ppb I)	10 ppm I_2/(1.0×10^{-1} ppb I)	10 ppm I_2/(1.0×10^{-0} ppb I)	10 ppm I_2/(1.0×10^{1} ppb I)	10 ppm I_2/(1.0×10^{2} ppb I)
$[Hg]/[Hg]_0$	1.0	0.955	0.69	0.166	0.0

dx.doi.org/10.1021/jp412654s | J. Phys. Chem. A XXXX, XXX, XXX−XXX

As in the case of chlorine, no conversion is obtained in the absence of bromine atoms, $\sim 10^{-1}$ ppb would be necessary to obtain ~45% conversion of mercury observed at Chang et al.'s experiments, and a total conversion is obtained when ~1 ppb Br atoms are added to the reaction system. Table 29 and Figure 14 represent the results of these calculations.

The iodine mechanism including the insertion reaction calculated at the M06-2X/aug-cc-pVTZ-PP level of theory was used. Results indicate that higher concentrations of I atoms are needed to effect conversion relative to chlorine and bromine. As in the case of chlorine and bromine, no conversion is obtained in the absence of iodine atoms, $\sim 5 \times 10^{-1}$ ppb would result in ~15% conversion of mercury observed at Yan et al.'s experiments, and total conversion is obtained when $\sim 10^{2}$ ppb I atoms are initially present in the reaction system. Table 30 and Figure 15 represent the results of these calculations

The modeling results confirm that very small concentrations of X atoms ($\sim 10^{-5}$–10^{2} ppb) serve to reproduce the experimental mercury loss observed.

SUMMARY

We find that a fundamentally based reaction mechanism and kinetic parameters found in the literature do not predict any significant formation of HgX_2 or loss of Hg under atmospheric conditions relative to that observed in the experimental studies. There is also no conversion that occurs when trying to reproduce the experimental data using the rate constants developed in this study (with thermodynamically consistent reverse reactions with pressure dependence for the chemical activation and dissociation reactions are incorporated), when the insertion reactions ($Hg + X_2 \rightarrow HgX_2$) are included. We support the calculated barriers for insertion by Peterson for Br_2[8] and Liu for Cl_2.[36] The presence of halogen atoms or active surfaces are needed to effect HgX_2 formation in the modeled experiments.

ASSOCIATED CONTENT

Supporting Information

Text giving a more detailed description of the discussed literature results in the introduction, tables listing the thermochemical data used in this study and the parameters used in the determination of the pressure and temperature dependence of rate constants, and figures showing the chemical activation results and the comparison between the results obtained by Chemaster and ChemRate. This material is available free of charge via the Internet at http://pubs.acs.org.

AUTHOR INFORMATION

Corresponding Author

*E-mail: Bozzelli@njit.edu. Tel.: +1 973 596 3459.

Notes

The authors declare no competing financial interest.

ACKNOWLEDGMENTS

We thank the Basque Government for partial funding.

REFERENCES

(1) U.S. EPA. *Fed. Regist.* **2013**, *78*, 38001–38005.
(2) Senior, C. L. Behavior of Mercury in Air Pollution Control Devices on Coal-Fired Utility Boilers; . *Power Production in the 21st Century: Impacts of Fuel Quality and Operations*, Engineering Foundation Conference, Snowbird, UT, USA, 2001.
(3) Streets, D. G.; Zhang, Q.; Wu, Y. Projections of Global Mercury Emissions in 2050. *Environ. Sci. Technol.* **2009**, *43*, 2983–2988.
(4) *Changing Metal Cycles and Human Health*; Life Sciences Research Reports 28; Nriagu, J. O., Ed.; Berlin, Germany, 1984.
(5) Lindqvist, O.; Rodhe, H. Atmospheric Mercury: A Review. *Tellus, Ser. B* **1985**, *37*, 136–159.
(6) Lodenius, M.; Laaksovirte, K. Mercury Content of Fungi in Helsinki. *Ann. Bot. Fenn.* **1979**, *16*, 208–212.
(7) Peterson, K. A.; Balabanov, N. B. Mercury and Reactive Halogens: The Thermochemistry of Hg + {Cl_2, Br_2, BrCl, ClO, and BrO}. *J. Phys. Chem. A* **2003**, *107*, 7465–7470.
(8) Peterson, K. A.; Balanov, N. B.; Shepler, B. C. Accurate Global Potential Energy Surface and Reaction Dynamics for the Ground State of $HgBr_2$. *J. Phys. Chem. A* **2005**, *109*, 8765–8773.
(9) Hynes, A. J.; Donohoue, D. L.; Goodsite, M. E.; Hedgecock, I. M. Our Current Understanding of Major Chemical and Physical Processes Affecting Mercury Dynamics in the Atmosphere and at the Air-Water/Terrestrial Interfaces. *Mercury Fate and Transport in the Global Atmosphere*; Springer: New York, 2009; pp 427–457.
(10) Selin, N. E.; Jacob, D. J.; Park, R. J.; Yantosca, R. M.; Strode, S.; Jaeglé, L.; Jaffe, D. Chemical Cycling and Deposition of Atmospheric Mercury: Global Constraints from Observations. *J. Geophys. Res.: Atmos.* **2007**, *112*, 1–14.
(11) Dibble, T. S.; Zelie, M. J.; Mao, H. Thermodynamics of Reactions of ClHg and BrHg Radicals with Atmospherically Abundant Free Radicals. *Atmos. Chem. Phys.* **2012**, *12*, 10271–10279.
(12) Goodsite, M. E.; Plane, J. M. C.; Skov, H. A Theoretical Study of the Oxidation of HgO to $HgBr_2$ in the Troposphere. *Environ. Sci. Technol.* **2004**, *38*, 1772–1776.
(13) Mao, H.; Talbot, R. W.; Sive, B. C.; Kim, S. Y.; Blake, D. R.; Weinheimer, A. J. Arctic Mercury Depletion and Its Quantitative Link with Halogens. *J. Atmos. Chem.* **2010**, *65*, 145–170.
(14) Obrist, D.; Tas, E.; Peleg, M.; Matveev, V.; Faïn, X.; Asaf, D.; Luria, M. Bromine-Induced Oxidation of Mercury in the Mid-Latitude Atmosphere. *Nat. Geosci.* **2011**, *4*, 22–26.
(15) Driscoll, C. T.; Mason, R. P.; Chan, H. M.; Jacob, D. J.; Pirrone, N. Mercury as a Global Pollutant: Sources, Pathways, and Effects. *Environ. Sci. Technol.* **2013**, *47*, 4967–4983.
(16) Ogg, R. A.; Martin, H. C.; Leighton, P. A. Kinetics of the Vapor Phase Reaction of Mercury and Halogens. *J. Am. Chem. Soc.* **1936**, *58*, 1922–1924.
(17) P'yankov, V. A. Kinetics of the Reaction between Mercury Vapor and Ozone. *Zhur. Obschev. Khim. (Russ. J. Gen. Chem.)* **1949**, *19*, 224–229.
(18) Menke, R.; Wallis, G. Detection of Mercury in Air in the Presence of Chlorine and Water Vapor. *Am. Ind. Hyg. Assoc. J.* **1980**, *41*, 120–124.
(19) Hall, B.; Lindqvist, O.; Ljungstrom, E. Mercury Chemistry in Simulated Flue Gases Related to Waste Incineration Conditions. *Environ. Sci. Technol.* **1990**, *24*, 108–111.
(20) Fontijn, A.; Hranisavljevic, R. J. Kinetics of Ground-State Cd Reactions with Cl_2, O_2, and HCl over Wide Temperature. *J. Phys. Chem. A* **1997**, *101*, 2323–2326.
(21) Schroeder, W. H.; Niki, H.; Yarwood, G. Transformation Processes Involving Mercury Species in the Atmosphere—Results from a Literature Survey. *Water Air Soil Pollut.* **1991**, *56*, 653–666.
(22) Kramlich, J. C.; Sliger, N.; Marinov, N. M. Towards the Development of a Chemical Kinetic Model for the Homogeneous Oxidation of Mercury by Chlorine Species. *Fuel Process. Technol.* **2000**, *65–66*, 423–438.
(23) Edwards, J. R.; Srivastava, R. K.; Kilgroe, J. D. A Study of Gas-Phase Mercury Speciation Using Detailed Chemical Kinetics. *J. Air Waste Manage. Assoc.* **2001**, *51*, 869–877.
(24) Kee, R. J. Senkin Manual. *Chemkin Collection*, Release 3.6; Reaction Design: San Diego, CA, USA, 2001.
(25) Ariya, P. A.; Khalizov, A.; Gidas, A. Reactions of Gaseous Mercury with Atomic and Molecular Halogens: Kinetics, Product Studies, and Atmospheric Implications. *J. Phys. Chem. A* **2002**, *106*, 7310–7320.
(26) Raofie, F.; Snider, G.; Ariya, P. A. Reaction of Gaseous Mercury with Molecular Iodine, Atomic Iodine, and Iodine Oxide Radicals—

Kinetics, Product Studies, and Atmospheric Implications. *Can. J. Chem.* **2008**, *86*, 811−820.
(27) Chang, S. G.; Miller, C.; Liu, S. H.; Yan, N. Q.; Liu, Z. R.; Qu, Z.; Wang, P. H. Using Bromine Gas to Enhance Mercury Removal from Flue Gas of Coal-Fired Power Plants. *Environ. Sci. Technol.* **2007**, *41*, 1405−1412.
(28) Chang, S. G.; Miller, C.; Yan, N. Q.; Liu, S. H. Method for the Study of Gaseous Oxidants for the Oxidation of Mercury Gas. *Ind. Eng. Chem. Res.* **2005**, *44*, 5567−5574.
(29) Yan, N.; Qu, Z.; Liu, P.; Chi, Y.; Jia, J. Bromine Chloride as an Oxidant to Improve Elemental Mercury Removal from Coal-Fired Flue Gas. *Environ. Sci. Technol.* **2009**, *43*, 8610−8615.
(30) Qu, Z.; Yan, N.; Liu, P.; Jia, J.; Yang, S. The Role of Iodine Monochloride for the Oxidation of Elemental Mercury. *J. Hazard. Mater.* **2010**, *183*, 132−137.
(31) Ariya, P. A.; Khalizov, A. F.; Virwanathan, B.; Larregaray, P. A Theoretical Study on the Reactions of Hg with Halogens: Atmospheric Implications. *J. Phys. Chem. A* **2003**, *33*, 6360−6365.
(32) Peterson, K. A.; Shepler, B. C.; Balabanov, N. B. Ab Initio Thermochemistry Involving Heavy Atoms: Investigation of the Reactions Hg + IX (X = I, Br, Cl, O). *J. Phys. Chem. A* **2005**, *109*, 10363−10372.
(33) Wilcox, J. A Kinetic Investigation of High-Temperature Mercury Oxidation by Chlorine. *J. Phys. Chem. A* **2009**, *113*, 6633−6639.
(34) Stevens, W. J.; Krauss, M.; Basch, H.; Jasien, P. G. Relativistic Compact Effective Potentials and Efficient, Shared-Exponent Basis Sets for the Third-, Fourth-, and Fifth-Row Atoms. *Can. J. Chem.* **1992**, *70*, 612−630.
(35) Wilcox, J.; Okano, T. Ab Initio-Based Mercury Oxidation Kinetics Via Bromine at Postcombustion Flue Gas Conditions. *Energy Fuels* **2011**, *25*, 1348−1356.
(36) Liu, J.; Yuan, J.; Qu, W.; Wang, S.; Qiu, J.; Zheng, C. Theoretical Studies of Properties and Reactions Involving Mercury Species Present in Combustión Flue Gases. *Energy Fuels* **2010**, *24*, 117−122.
(37) Fry, A. R.; Cauch, B.; Lighty, J. S.; Senior, C. L.; Silcox, G. D. Experimental Evaluation of the Effects of Quench Rate and Quartz Surface Area on Homogeneous Mercury Oxidation. *Proc. Combust. Inst.* **2007**, *31*, 2855−2861.
(38) Hutson, N. D. Mercury Capture on Fly Ash and Sorbents: The Effects of Coal Properties and Combustion Conditions. *Water Air Soil Pollut.* **2008**, *8*, 323−331.
(39) Niksa, S.; Fujiwara, N.; Helble, J. J. Kinetic Modeling of Homogeneous Mercury Oxidation: The Importance of NO and H_2O in Predicting Oxidation in Coal-Derived Systems. *Environ. Sci. Technol.* **2001**, *35*, 3701−3706.
(40) Qiu, J.; Helble, J. J.; Sterling, R. O. Development of an Improved Model for Determining the Effects of SO_2 on Homogeneous Mercury Oxidation. *Proceedings of the 28th International Technical Conference on Coal Utilization & Fuel Systems*; Coal Technologies Associates: North Potomac, MD, USA, 2003.
(41) Schofield, K. Fuel-Mercury Combustion Emissions: An Important Heterogeneous Mechanism and an Overall Review of Its Implications. *Environ. Sci. Technol.* **2008**, *42*, 9014−9030.
(42) Senior, C. L.; Helble, J. J.; Mamani-Paco, R.; Sarofim, A. F.; Zeng, T. Gas-Phase Transformations of Mercury in Coal-Fired Power Plants. *Fuel Process. Technol.* **2000**, *63*, 197−213.
(43) Widmer, N. C. Practical Limitation of Mercury Speciation in Simulated Municipal Waste Incinerator Flue Gas. *Combust. Sci. Technol.* **1998**, *134*, 315−326.
(44) Widmer, N. C.; West, J.; Cole, J. A. Thermochemical Study of Mercury Oxidation in Utility Boiler Flue Gases. *Proceedings of the Air & Waste Management Association 93rd Annual Conference and Exhibition*, Salt Lake City, UT, USA; Air & Waste Management Association: Pittsburgh, PA, USA, 2000.
(45) Xu, M.; Qiao, Y.; Zheng, C.; Li, L.; Liu, J. Modeling of Homogeneous Mercury Speciation. *Combust. Flame* **2003**, *132*, 208−218.
(46) Peterson, K. A.; Shepler, B. C. Mercury Monoxide: A Systematic Investigation of Its Ground Electronic State. *J. Phys. Chem. A* **2003**, *107*, 1783−1787.
(47) NIST-JANAF Themochemical Tables, 4th ed. *J. Phys. Chem. Ref. Data*; American Chemical Society: Washington, DC, USA, 1998; Monograph *9*; pp 1−1951.
(48) Becke, A. D. A New Mixing of Hartree-Fock and Local Density-Functional Theories. *J. Chem. Phys.* **1993**, *98*, 1372−1377.
(49) Hamprecht, F. A.; Cohen, A. J.; Tozer, D. J.; Handy, N. C. Development and Assessment of New Exchange-Correlation Functionals. *J. Chem. Phys.* **1998**, *109*, 6264−6272.
(50) Chai, J. D.; Head-Gordon, M. Systematic Optimization of Long-Range Corrected Hybrid Density Functionals. *J. Chem. Phys.* **2008**, *128*, 40−55.
(51) Grimme, S. Semiempirical Hybrid Density Functional with Perturbative Second-Order Correlation. *J. Chem. Phys.* **2006**, *124*, 67−83.
(52) Zhao, Y.; Truhlar, D. G. The M06 Suite of Density Functionals for Main Group Thermochemistry, Thermochemical Kinetics, Noncovalent Interactions, Excited States, and Transition Elements: Two New Functionals and Systematic Testing of Four M06-Class Functionals and 12 Other Functionals. *Theor. Chem. Acc.* **2008**, *120*, 215−241.
(53) *Advances in Chemical Physics*; Cizek, J., Ed.; Wiley Interscience: New York, 1969; Vol. *14*.
(54) Purvis, G. D., III; Bartlett, R. J. A Full Coupled-Cluster Singles and Doubles Model—The Inclusion of Disconnected Triples. *J. Chem. Phys.* **1982**, *76*, 1910−1918.
(55) Scuseria, G. E.; Janssen, C. L.; Schaefer, H. F., III. An Efficient Reformulation of the Closed-Shell Coupled Cluster Single and Double Excitation (Ccsd) Equations. *J. Chem. Phys.* **1988**, *89*, 7382−7387.
(56) Scuseria, G. E.; Schaefer, H. F., III. Is Coupled Cluster Singles and Doubles (Ccsd) More Computationally Intensive Than Quadratic Configuration-Interaction (Qcisd)? *J. Chem. Phys.* **1989**, *90*, 3700−3703.
(57) Pople, J. A.; Head-Gordon, M.; Raghavachari, K. Quadratic Configuration Interaction—A General Technique for Determining Electron Correlation Energies. *J. Chem. Phys.* **1987**, *87*, 5968−5975.
(58) Peterson, K. A.; Puzzarini, C. Systematically Convergent Basis Sets for Transition Metals. II. Pseudopotential-Based Correlation Consistent Basis Sets for the Group 11 (Cu, Ag, Au) and 12 (Zn, Cd, Hg) Elements. *Theor. Chem. Acc.* **2005**, *114*, 283−296.
(59) Peterson, K. A.; Figgen, D.; Goll, E.; Stoll, H.; Dolg, M. Systematically Convergent Basis Sets with Relativistic Pseudopotentials. I. Correlation Consistent Basis Sets for the Post-D Group 13−15 Elements. *J. Chem. Phys.* **2003**, *119*, 11113−11127.
(60) Figgen, D.; Rauhut, G.; Dolg, M.; Stoll, H. Energy-Consistent Pseudopotentials for Group 11 and 12 Atoms: Adjustment to Multiconfiguration Dirac-Hartree-Fock Data. *Chem. Phys.* **2005**, *311*, 227−244.
(61) Hay, P. J.; Wadt, W. R. Ab Initio Effective Core Potentials for Molecular Calculations. Potentials for the Transition Metal Atoms Sc to Hg. *J. Chem. Phys.* **1985**, *82*, 270.
(62) Häussermann, U.; Dolg, M.; Stoll, H.; Preuss, H.; Schwerdtfeger, P.; Pitzer, R.M. Accuracy of Energy-Adjusted Quasirelativistic *ab Initio* Pseudopotentials. All-Electron and Pseudopotential Benchmark Calculations for Hg, HgH and Their Cations. *Mol. Phys.* **1993**, *78*, 1211.
(63) Schwerdtfeger, P.; Dolg, M.; Schwarz, W. H. E.; Bowmaker, G. A.; Boyd, P. D. W. The Baldet−Johnson (B2σ+ −A2πi) System of 13c18o +. *J. Chem. Phys.* **1989**, *91*, 1762.
(64) Wedig, U.; Dolg, M.; Stoll, H.; Preuss, H. *Quantum Chemistry: The Challenge of Transition Metals and Coordination Chemistry*; Kluwer: Dordrecht, Holland, 1986.
(65) Frisch, M. J.; Trucks, G. W.; Schlegel, H. B.; Scuseria, G. E.; Robb, M. A.; Cheeseman, J. R.; Montgomery, J. A., Jr.; Vreven, T.; Kudin, K. N.; Burant, J. C.; et al. *Gaussian03*; Gaussian.: Wallingford, CT, USA, 2003.

(66) Frisch, M. J.; Trucks, G. W.; Schlegel, H. B.; Scuseria, G. E.; Robb, M. A.; Cheeseman, J. R.; Scalmani, G.; Barone, V.; Mennucci, B.; Petersson, G. A.; et al. *Gaussian 09*, Revision A.1. Gaussian: Wallingford, CT, USA, 2009.
(67) Sheng, C.; Bozzelli, J. W.; Chang, A. Y.; Dean, A. M. Detailed Kinetics and Thermochemistry of $C_2H_5 + O_2$: Reaction Kinetics of the Chemically-Activated and Stabilized $CH_3CH_2OO^{\bullet}$ Adduct. *J. Phys. Chem. A* **2002**, *106*, 7276−7293.
(68) Mokrushin, V.; Bedanov, V.; Tsang, W.; Zachariah, M. R.; Knyazev, V. D.; McGivern, W. S., *ChemRate Technology*; Mokrushin Software and National Institute of Standards and Technology: Gaithersburg, MD, USA, 2011.
(69) Mokrushin, V.; Tsang, W.; *ChemRate 1.5.8*; Mokrushin Software and National Institute of Standards and Technology: Gaithersburg, MD, USA, 2009.
(70) Widman, R. P.; DeGraff, B. A. On the Gas-Phase Recombination of Chlorine Atoms. *J. Phys. Chem. A* **1973**, *77*, 1325−1328.
(71) Baulch, D. L.; Duxbury, J.; Grant, S. J.; Montague, D. C. . Evaluated Kinetic Data for High Temperature Reactions, Vol. 4: Homogeneous Gas Phase Reactions of Halogen- and Cyanide-Containing Species. *Journal of Physical and Chemical Reference Data*; 1981; Vol. *10*.
(72) Baulch, D. L.; Duxbury, J.; Grant, S. J.; Montague, D. C. Evaluated Kinetic Data for High Temperature Reactions. Vol. 4: Homogeneous Gas Phase Reactions of Halogen- and Cyanide-Containing Species. *J. Phys. Chem. Ref. Data* **1981**, *10*, 723.
(73) *Comprehensive Inorganic Chemistry*; Aylett, B. J., Ed.; Pergamon Press: Elmsford, NY, USA, 1973; Vol. *3*.
(74) Bell, S.; McKenzie, R. D.; Coon, J. B. The Spectrum of $HgCl_2$ in the Vacuum Ultraviolet. *J. Mol. Spectrosc.* **1966**, *20*, 217−225.
(75) Adams, D. M.; Hills, D. J. J. Single-Crystal Infrared Study and Assignment for Mercury(II) Chloride and Bromide. *J. Chem. Soc., Dalton Trans.* **1978**, 776−782.
(76) Chase, M. W., Jr.; Davies, C. A.; Downey, J. R.; Frurip, D. J.; McDonald, R. A.; Syverud, A. N. *J. Phys. Chem. Ref. Data*; American Chemical Society: Washington, DC, USA, 1985; Monograph *14*.
(77) Bermejo, D.; Jimenez, J. J.; Martinez, R. Z. J. The Stretching Fundamental Bands of $^{35}Cl_2$, $^{37}Cl_2$ and $^{35}Cl^{37}Cl$. *J. Mol. Spectrosc.* **2002**, *212*, 186−193.
(78) Stroemberg, D.; Gropen, O.; Wahlgren, U. Non-Relativistic and Relativistic Calculations on Some Zn, Cd and Hg Complexes. *Chem. Phys.* **1989**, *133*, 207−219.
(79) Kaupp, M.; Vonschnering, H. G. The Dominance of Linear 2-Coordination in Mercury Chemistry: Quasirelativistic and Non-relativistic ab Initio Pseudopotential Study of $(HgX_2)_2$ (X = F, Cl, Br, I, H). *Inorg. Chem.* **1994**, *33*, 2555−2564.
(80) Givan, A.; Loewenschuss, A. The Infrared and Raman Spectra of Matrix Isolated Binary and Mixed Mercury Halides. *J. Chem. Phys.* **1976**, *64*, 1967−1972.
(81) Clark, R. J. H.; Rippon, D. M. Vapour Phase Raman Spectra of Mercury(II) Chloride, Mercury(II) Bromide and Mercury(II) Iodide. V1(Σ) Band Contours and the Mercury-Halogen Bond Polarisability Derivatives. *J. Chem. Soc., Faraday Trans. 2* **1973**, *69*, 1496−1501.
(82) Spiridonov, V. P.; Gershikov, A. G.; Butayev, B. S. Molecular Structure and Vibrational Potential Function of HgI_2: Electron Diffraction Study. *J. Mol. Struct.* **1979**, *52*, 53−62.
(83) Martin, F.; Bacis, R.; Churassy, S.; Verges, J. Laser-Induced-Fluorescence Fourier Transform Spectrometry of the XO_g^+ State of I_2: Extensive Analysis of the $BO_u^+ \rightarrow XO_g^+$ Fluorescence Spectrum of $^{127}I_2$. *J. Mol. Spectrosc.* **1986**, *116*, 71−100.
(84) Deyanov, R. Z.; Petrov, K. P.; Ugarov, V. V.; Shchedrin, B. M.; Rambidi, N. G. Automatic Background Subtraction in Gas Electron Diffraction: The Covariance Matrix in Least-Squares Structure-Parameter Analysis. *Zh. Strukt. Khim. (J. Struct. Chem.)* **1985**, *26*, 698−703.
(85) Huber, K. P., Herzberg, G. *Molecular Spectra and Molecular Structure. IV. Constants of Diatomic Molecules*; Van Nostrand Reinhold: Princeton, NJ, USA, 1979.
(86) Tellinghuisen, J.; Ashmore, J. G. The B→X Transition in $^{200}Hg^{79}Br$. *Appl. Phys. Lett.* **1982**, *40*, 867−869.
(87) *Electronic Spectra of Polyatomic Molecules*; Sponer, H., Teller, E., Eds.; American Physical Society: Ridge, NY, USA, 1941; Vol. *13*, p 96.
(88) Malt'sev, A. A.; Selivanov, G. K.; Yampolsky, V. I.; Zavalishin, N. I. Far Infrared Absorption Spectra of Mercury Dihalide Vapours. *Nat. (London), Phys. Sci.* **1971**, *231*, 157−158.
(89) Braune, H.; Engelbrecht, G. Z. Pseudooptical Absorption Spectra in $HgCl_2$ and $HgBr_2$. *Z. Phys. Chem., Abt. B* **1932**, *19*, 303.
(90) Focsa, C.; Li, H.; Bernath, P. F. Characterization of the Ground State of Br_2 by Laser-Induced Fluorescence Fourier Transform Spectroscopy of the $B^3\Pi_{0^+u}-X^1\Sigma^+_g$ System. *J. Mol. Spectrosc.* **2000**, *200*, 104−119.
(91) Beattie, I. R.; Horder, J. R. Gas-Phase Raman Spectra of Some Dihalides of Zinc and Mercury, of '$GaCl_2$' and $GaCl_2Br$ and $GaBr_2Cl$. *J. Chem. Soc. A* **1970**, *14*, 2433−2435.
(92) *NIST Standard Reference Database 25, Structure and Properties*, Version 2.02; National Institute of Standards and Technology: Gaithersburg, MD, USA, 1994.